OFF-LINE SIGNATURE VERIFICATION

NGUYEN THI MINH NGUYET

A THESIS SUBMITTED IN PARTIAL FULFILLMENT

OF THE REQUIREMENT FOR THE DEGREE OF

MASTER OF ENGINEERING IN COMPUTER ENGINEERING

INTERNATIONAL COLLEGE

KING MONGKUT'S INSTITUTE OF TECHNOLOGY LADKRABANG

BANGKOK 2012

KMITL-2012-IC-M-006-002

Thesis title	Off-line signature verification
Student	Ms. Nguyen thi Minh Nguyet
Student ID	53601155
Degree	Master of Engineering
Program	Computer Engineering
Year	2012
Thesis advisor	Asst.Prof.Dr. Pitak Thumwarin

Abstract

Biometrics is the automatic authentication technique based on human physical or behavioral characteristics. Face recognition, iris recognition and fingerprint recognition are based on physical characteristics, and voice recognition, gesture recognition while signature verification is based on behavioral characteristics. There are several advantages of biometrics over other types of security methods e.g. key cards and passwords, the former requires no memorizing and is difficult to be stolen. Therefore, biometrics is highly reliable a large of applications and can meet the high security requirements.

Off-line signature verification is a type of biometrics which will be discussed in this thesis. The off-line signature verification has been employed in wide variety of applications in many countries, especially in fund transfer of million people, bank checks, credit cards and in legal documents. This motivates us to pursue off-line signature verification for forensic purposes.

In this work, the preprocessing has first been performed to eliminate the noise from the scanned signature image from which the features of signatures are extracted. The obtained signing features are determined according to the methods relevant to the texture of off-line signature images. Finally, verification feature vectors are determined to verify whether the signatures are genuine and forged.

The study has been carried out on the GPDS300GRAY public database consisting of 253 signers, each of whom contains 24 genuine signatures and 30 forged signatures. The entire signature database thus comprises 6072 genuine signatures and 7590 forged signatures.

Although, there are several works employing the identical public database, our proposed methods include finite impulse response (FIR) system characterizing gray level change of signature, gray level occurrence matrix, Gabor filters and local phase quantization(LPQ) which have been applied for off-line signature verification. These proposed methods have improved the performance and efficiency of off-line signature verification over other methods on the same standard database. The better error rates are achieved in comparison with other works on the same database. Moreover, the time consumption of each method is investigated to locate the most effective one under the time constraints. Ultimately, it could possibly be concluded that LPQ is the most effective method in case of error rates.

TABLE OF CONTENT

LIST OF TABLES

LIST OF FIGURES

ACKNOWLEDGEMENTS

This thesis is the outcome of my 2 year work and completed with the support from many people and resources.

First of all, my sincere thanks to Assistant Professor Dr. Pitak Thumwarin for his dedication to his student and patience in assisting me with this thesis. I appreciate his valuable advices and effort during the course of my work. In addition, I would also like to thank my co-advisor Professor Takenobu Matsuura from Tokai University for his useful lectures and suggestions for my research.

Special thanks for my scholarship from Japan International Cooperation Agency (JICA) under AUN/SEEDNet project for sponsoring my studying in King Mongkut's Institute of Technology Ladkrabang (KMITL). Besides, I would also like to thank lecturers and staff in International College in KMITL as well with their lectures and corporation during my study period.

Special thanks to my roommate, my lab mate and other friends in KMITL, I appreciate their friendship and sympathetic help which have made my life here much easier.

Lastly, I would like to thank my mother and my family in Vietnam for their enormous encouragement and assistance. Without them, my work here would be impossible.

Bangkok, Thailand

2012

Nguyen thi Minh Nguyet

Chapter 1

Introduction

1.1 Background

1.1.1 Biometrics

Biometrics is an automatic identification of a person based on his/her anatomical (e.g. finger print, iris) or behavioral (e.g. signature) characteristics or traits. This method of identification possesses several advantages over the traditional methods of ID cards (tokens) or PIN (passwords) in that: (1) The person to be identified is required to be physically present at the point of identification and (2) identification based on biometrics techniques removes the requirement to memorize the password or carry the token keys. Modern lifestyles and the need to safeguard personal sensitive data necessitate the greater use of biometrics. Biometrics can potentially prevent unauthorized access to ATMs, cell phones, laptops, computer networks and certain sensitive documents. PINs, token keys, or passwords may be forgotten, stolen or lost; however, these issues could be solved with biometrics. Consequently, biometric systems are being improved to enhance security while reducing the financial frauds. Fingerprints, palm or hand geometry, retina, facial characteristics are examples of common physical biometrics, while signature verification and voice recognition belong to behavioral biometrics. Depending upon the applications, the biometric systems can function on either verification or recognition.

1.1.2 Verification and recognition

It is necessary to classify between verification systems and recognition systems. A verification system merely classifies whether a particular entity belongs to a specific class, whereas a recognition system has to choose to which certain class the identity belongs. Moreover, the recognition system can classify multiple classes, while the verification system is used for two-class classifier. The main focus of this thesis is on off-line signature verification in which the images of off-line signatures are studied.

1.1.3 Off-line signature verification

A signature is a kind of biometrics related to behavior of people because, unlike fingerprint, iris, or face, it is not a physical part of human beings but a behavior. Therefore, it may have changed over time and may not be the same every time the signature is signed. Signature verification analyzes the way people sign their names and the significant features of their signatures, such as speed, velocity, and pressure (Simon Liu, 2001). The hand-written signature is widely accepted personal attributes for identity verification. Compared with other biometrics (e.g., fingerprint, face, voice, retina and iris scanning), signature verification has a number of advantages. First, signature analysis can be applied only when the signature owner is conscious and willing to write in the usual manner; although in some special situations a person may be forced to submit the hand writing sample but this issue is out of our scope in this thesis. Forging a signature is deemed to be more difficult than forging a fingerprint. Furthermore, a fingerprint may be used when the person is unconscious or intoxicated.

Unfortunately, signature verification is a difficult discrimination problem since a hand-written signature is the result of a complex process depending on the physical and psychological conditions of the signers as well as the condition of the signing process. Off-line signature or static signature is merely a 2-dimension image of signature; thus, researchers on off-line signature verification lack the dynamic characteristics of signatures inherent in on-line signature verification. In addition, the off-line signatures may contain many noises and less information due to a lack of dynamic information of the pen-tip movements, such as pen-tip coordinates, pressure, velocity, acceleration, pen-up, and pen-down, all of which can be recorded real time in tablets but not in an image scanner.

The observation and experience indicate that signatures vary by country, age, time, habits, psychology, and practical conditions. Another challenge of off-line signature verification is that one same authentic person may sign in a variety of ways, thus making verification between genuine and forged signatures increasingly difficult.

Figure 1.1 shows an example of signature of Charles Dickens which had changed during his life. When he was young, his signature was bolder and stressed, but later when he was older, his signature was thinner and weaker.

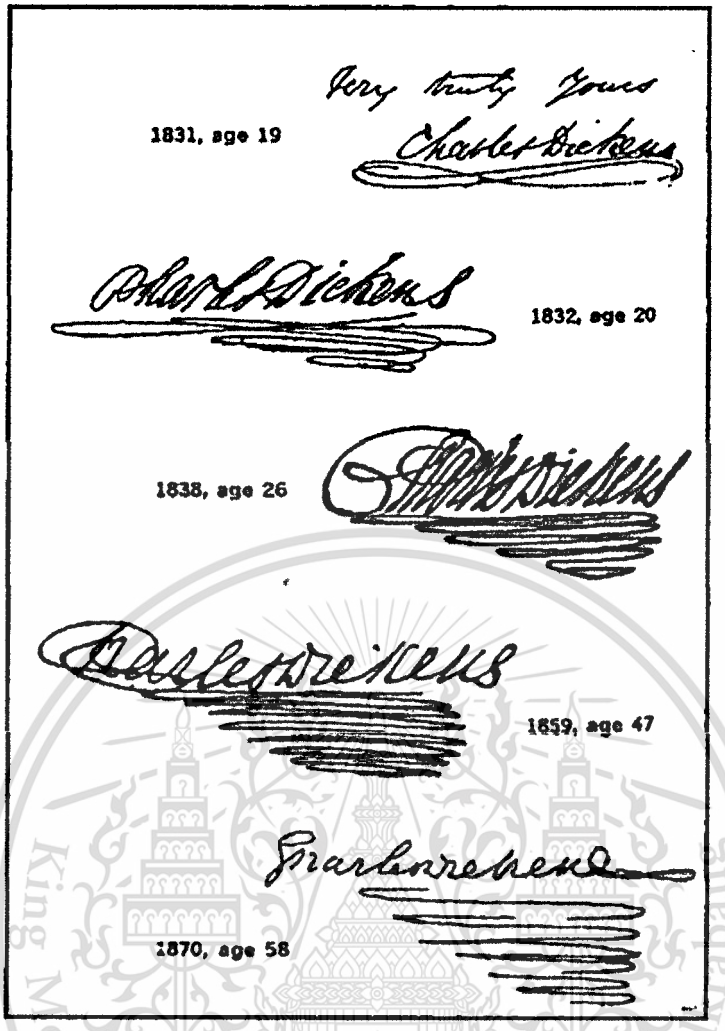

Figure 1.1 The change of signature at different stages of life. In his 20's, Charles Dickens's signature was bold and forceful. When he became older, his signature was smaller and weaker. This characteristic could be noticed over the years (Abbas, 1994).

However, off-line signature verification systems have a significant advantage in that they do not require special processing devices when signatures are produced. In fact, the accuracy of off-line verification system is emphasized; thus, the off-line signature verification possesses many more applications than does the on-line verification systems. Off-line signature verification applications for cash, cheque are typical examples. In this sense, off-line signature verification has interested a great number of researchers who recognize its valuable applications. Since no doubts automatic off-line signature verification has a very important role in the set of biometric techniques for personal verification (J. F. Vargas M. F., 2010). Consequently, the number of researchers who study feature extraction methodology of off-line signature verification has been increased recently (S. Lee, 1992).

Two major approaches to studying off-line signature verification are the static and pseudo-dynamic approaches. The former involves geometric measures of the signature while the latter attempts to determine dynamic information from the static image. Statistical texture analysis requires the computation of texture features from statistical distribution of observed combinations of intensities at specified positions relative to each other in an image. Dynamic information cannot be directly derived from static signature images. Instead, certain features that partly represent dynamic information can be derived. These special characteristics are referred to as pseudo-dynamic information, which can be reconstructed from the static images (J. F. Vargas M. F., 2010). Another point that researchers on off-line signature verification should need is that on-line signature verification uses special input devices such as tablets, while off-line signature systems are much more difficult because the only available information is the static two-dimensional images obtained by scanning pre-written signatures. On the contrary, the dynamic information can be captured real-time on a tablet but not by an image scanner. Furthermore, the off-line signature verification method requires complex image processing techniques to segment and analyze signature shape for feature extraction, thereby rendering the on-line signature verification more promising. An increasing amount of research has focused on feature-extraction methodology for off-line signature verification (S. Lee, 1992).

If researchers work on different databases, it will be difficult to compare the performances of several methods of off-line signature verification. Using a standard database, the performance among methods could be compared. These issues will further be discussed in this thesis.

1.1.4 Forged signature classification

According to work of (Panton, 2010), there exist three types of forged signatures as classified by increasing order of forgery quality. First, a random forgery is produced by an individual who has no prior knowledge of (or is making no attempt to imitate) the appearance of the authentic signature nor knowledge of the authentic name. A genuine signature belongs to a certain person, whereas others are forgeries. The second type of forged signature is casual signature by forgers who possess some information of the victim such as name and surname, but have no information about how the real

signature appears. The third type is the one forged by skilled forgers who not only know the person but also how his/her signature is signed.

Skillfully forged signatures can be classified into 2 main types: amateur forgeries and professional forgeries. Amateur forged signatures are generated by those who have accessed one or more copies of genuine signatures and have unlimited time to mimic their signatures. Professional forgeries are created by a person who has knowledge about authentic handwriting and authentic signatures, thus able to imitate the authentic signatures with great precision. Professional forged signatures are difficult to detect by both humans and machines because the forged ones are closely identical to the authentic signatures. Therefore, working on professional signatures means working with the most challenging forgers for researchers.

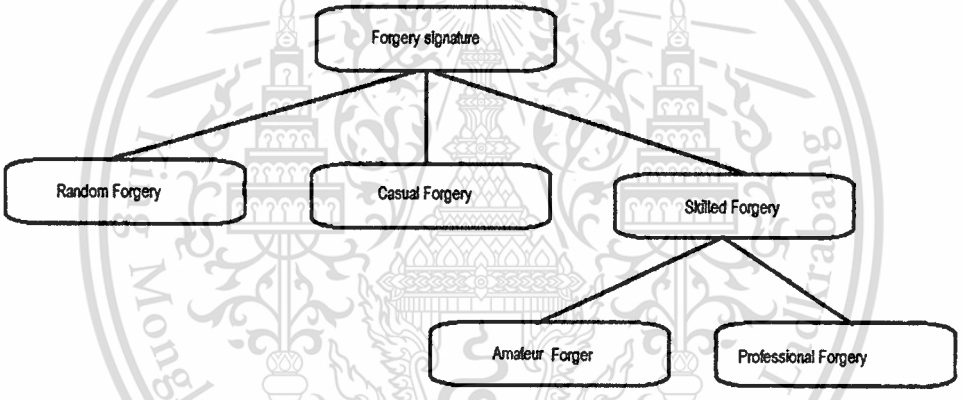

Figure 1.2 Forged signature classifications.

Figure 1.2 illustrates forged signatures which can be broken down into particular types. In some works, researchers may apply their methods for one forged type, or two types of forgers. In this work, we have studied on amateur forgeries which are retrieved from public database.

1.2 Related works

Advance in current technology requires the use of off-line signature verification for many real applications, examples of which are credit card transactions, document flow applications, and identity authentication prior to access to sensitive information. There exist several studies on off-line signature verification with some works studying the geographic of signatures while other works on the texture of signatures.

In the work of (J. Ruiz-del-Solar C. D., 2008) based on the wide baseline matching methodology, the local interest points are computed in the neighborhood of these points, and then these descriptors are compared using local and global matching procedures. For each user, a Naïve Bayes classifier of the proposed signature verification system was trained using the Weka package and 10-fold cross-validation. Previously, for each classification the relevant features were automatically selected by using Weka. For their work, they used GPDS database (J.F Vargas, 2007) and the final results were false reject rate (FRR) of 16.4%, false accept rate (FAR) of 14.2%.

The work of (R. Larkins, 2008) introduced Adaptive Feature Thresholding (AFT) which is a novel method of person-dependent off-line signature verification. Their method enhanced how a simple image feature of a signature was converted to a binary feature vector by signification improving its representation in relation to the training signatures. The researcher then calculated the similarity between signatures by their corresponding binary feature vectors. The evaluation of AFT was carried out on two datasets: CEDAR and GPDS (J.F Vargas, 2007). In the case of CEDAR dataset, the best obtained result was by manual AFT with 92.58% accuracy, while that of GPDS, the accuracy was 89.79% with the same method.

The work of (B.H. Shekar, 2011) proposed a model involved in two major phrases: preprocessing and eigen-signature construction for the training system. In the preprocessing stage, the signature images were binarized to remove the complex background. Afterward, the shapes obtained due to preprocessing were considered for the purpose of Eigen-signature construction where by each shape results in a matrix containing intensity values. The appearance-based paradigm was applied to extract features and each signature was presented in a matrix form before being converted into vector form. The experiments were conducted on the Kannada offline signature database to exhibit the performance, and the efficiency of the method was 14.33% and 8.78% with 15 training samples.

The work of (M.B Yilmaz, 2011) presented an offline signature verification system based on a signature's local histogram features. The signature was divided into zones using both the Cartesian and polar coordinate systems and two different histogram features which were calculated for each zone: histogram of oriented gradients (HOG) and histogram of local binary patterns (LBP). The GPDS-300

public database was used with the first 160 users of the database used in testing while the remaining users, i.e., 161 to 300, from the GPDS-300 dataset used in training. The performance of their methods was shown by HOG features obtained using Polar coordinates (HOG-Polar) with 19.58% error rate using user-dependent support vector machine (USVM). The local binary pattern (LBP) had the 19.84% error rate.

The work of (J. F. Vargas M. F., p. 2010) and (M. A. Ferrer, 2010) proposed method based on pseudo-dynamic features. A study by (J. F. Vargas M. F., 2010) applied the statistical texture analysis which requires the computation of texture features from the statistical distribution of observed combinations of intensities at specified positions relative to each other in an image. Biometric systems based on signature verification in conjunction with texture analysis can reveal information about ink-pixels distribution, which reflects personal characteristics of the signers, i.e., pen-holding, writing speed, and pressure. Their approaches were gray level co-occurrence matrix and local binary pattern (LBP) which relate to texture analysis. LBP operator describes the surrounding of each pixel by generating a bit-code from the binary derivatives of the pixel as a complementary measure for local contrast. In their experiments, two datasets are employed in this work: GPDS-100 and MCYT. The experimental results for skilled forgeries show that using grey level information achieves reasonable system performance with equal error rates of 16.27% and 12.82%.

1.3 Motivations and objectives

1.3.1 Realistic problems

A variety of applications require the off-line signature verification for forensic purposes. A typical example for off-line signature verification is the issue of cheque fraud(Authority). This happens when criminals steal cards of authentic people, or they obtain authentic cards or account details, this also means criminals to steal money from authentic accounts. If it occurs, authentic people will see unfamiliar transactions on their statements or suddenly notice that they have exceeded their overdraft and their cards are refused when they try to make a purchase. There are some facts and statistics about check fraud (fraud, 2012).

According to BankInforSecurity's 2012 Facts of Fraud Survey, check fraud is the second most common scheme that institutions face, placing just behind payment card fraud. Approximately 76% of banks ranked check fraud second among the top fraud threats they faced in 2011. Based on a December 2011 survey published by the *American Bankers Association(ABA)*, 73 percent of banks reported check fraud losses in 2010, totaling approximately $893 million in losses. *American Banker's Association, 2011*: The 2009 ABA study estimated that there were 760,955 cases of check fraud in 2008 with actual losses estimated at $1.024 billion, compared to 561,306 cases and $969 million in 2005 (2006 ABA study) and 616,469 cases and $677 million in 2002 (2003 ABA study). Counterfeit checks resulted in a loss of $271 million for banks in 2006, a 160% increase from 3 years prior.

There are several applications on this field like cheque check, cash check in which authentic signatures are used to verify genuine people.

There are several methods to deal with fraud check in reality, one of which is off-line signature verification. Another application of off-line signature verification is cash signature check, an example of which is shown in Figure 1.3.

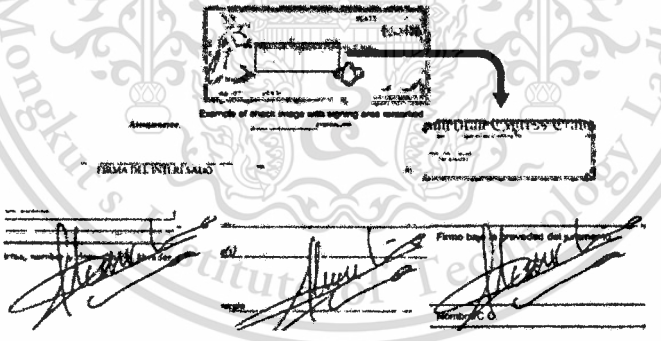

Figure 1.3 An application of off-line signature verification (M. A. Ferrer J. F., 2012).

1.3.2 Goals of the research

The thesis is motivated by the requirement of potential benefits for automatic signature verification systems such as authentic login systems, document off-line signature verification, etc.

The objective of this thesis is to investigate the process which automatically verifies handwritten off-line signatures. In other words, this process will be responsible to classify authentic or forged signature with effective performance of off-line signature verification. Moreover, the goal of this research is

applying texture analysis for off-line signature verification and emphasizing on investigating the feature extraction of the texture analysis on off-line signature images. Furthermore, the comparisons among methods deal with genuine and forged discrimination and some related works on the same database will be presented.

In this thesis, the four methods are introduced to extract the individual features of handwriting. First the FIR system characterizing gray level change of off-line signature image is introduced. The obtained impulse responses of the FIR systems are used as the individual feature of handwriting. In this case, the off-line signature verification problem can be reduced to system identification problem. The second method is gray level change occurrence matric (GLCM), and its features will be used as the off-line handwriting features. Third method Gabor filter features is used to verify genuine and forgery signatures. Lastly, local phase quantization is applied to verify off-line signature images and extracted the off-line handwriting features.

1.4 Off-line signature verification process

In this thesis, we will show an overview of our entire process. There are 5 main steps in our process, i.e., data acquisition, preprocess, feature extraction, off-line signature verification, and experimental results. The details of each step will be further presented in the remaining of this thesis.

Preprocessing is the process by which noise in off-line signature images is eliminated to gain the better quality images for later steps and to obtain better performances. Feature extraction is responsible for extracting the individual characteristics of each signature and to distinguish among off-line signature images. The feature vectors of each off-line signature are extracted in the verification step. The final step is experiments with which the results from verification engine will be verified, based on the dissimilarity between the test and the reference set signatures.

Figure 1.4 shows an overview of our off-line signature process from the first step data acquisition to experiments. This figure provides a general view of our off-line signature verification process in this thesis.

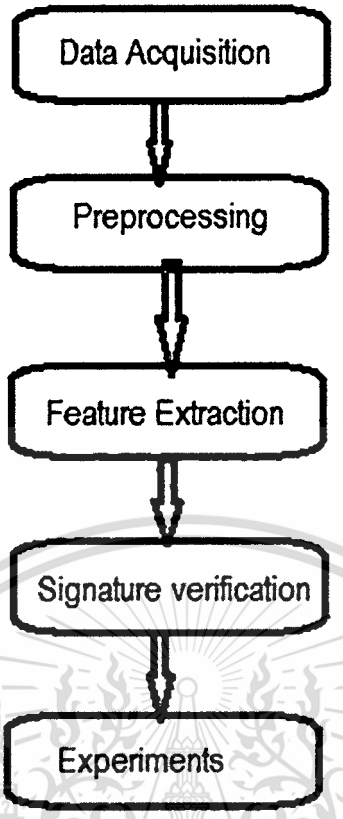

Figure 1.4 Off-line signature verification process.

1.5 Outline of the thesis

Chapter 1: Background or literature review provides the background information for this thesis and an overview of off-line signature verification with its statistical, structural approaches. Works related to this research together with their reviews are presented in this chapter. The main goal and objectives are also mentioned in this section.

In this chapter, we have introduced the definition of biometrics in general and given an overview of off-line signature. The advantage and challenges of off-line signature verification over other biometrics are shown. Moreover, this chapter shows the difference between recognition and verification, and the concentration of texture analysis on off-line signature verification in this thesis as well. The classifications of forged signatures are indicated.

Chapter 2: In this chapter, we will show our data acquisition and preprocessing process for off-line signatures in our database. The preprocessing of our off-line signature process will be also presented as starting phase of off-line signature verification.

Chapter 3: This chapter reviews general theories which will be applied to off-line signature verification. Design of experiments explains the process undertaken in designing, preparing, and conducting the feature extractions.

Chapter 4: Results and comparisons drawn from the experiments are listed and analyzed. The testing result of the designed networks for all subjects is listed in separate sections.

Chapter 5: General conclusions, discussions and suggestions for future work are presented.

Chapter 2

Preprocessing

2.1 Data acquisition

This work has employed the GPDS300 public database from the Digital Signal Processing Group de Las Palmas de Gran Canaria (ULPGC-Spain). The database is extracted from the GPDS-960 signature corpus which contains 24 genuine and 30 forged signatures. The genuine signatures were taken in one session since organization of a vast number of people in various sessions. The signers filled up a form for 24 boxes of different sizes. Each forger form contains 5 images of different genuine signatures chosen randomly. The forger could imitate each one of the 5 signatures. Forgers were taken as long as they like to learn the signature and perform the forgeries. The entire process of signing was accomplished under the supervision of an operator (J.F Vargas, 2007).

A form was created in order to collect the genuine signatures corresponding to each individual. The form contains 24 boxes, inside which signatures should be written. The boxes approximate the usual size of the provided spaces on official documents, e.g., checks and credit card vouchers. Of the 24 boxes there are two sizes of boxes: the larger boxes are of 5 x 3.5 cm in width and height while the smaller ones 5.5 x 2.5cm in width and height. The signers were asked not to sign outside the frame of the boxes.

The forms to collect forgeries contain 5 randomly chosen genuine signatures to be forged. Each genuine signature would be forged 3 times in the boxes below the respective genuine signature. Similar to the form of genuine signatures, there are forms with large boxes and those with small boxes. The forms were designed taking into account two simple rules: the five signatures to forge are of different signatures.

Following the collection of the signature forms, each form was scanned with HP4400 device using 256 level gray scale and 300pp resolution. Once scanned, the images were converted to black and white using a fixed image threshold equal to 230. Gray scale images were kept in order to deal with

approaches using that information. (J. F. Vargas M. A., 2007). GPDS3000GRAY signature database consists of 6072 genuine signatures and 7590 forgeries, all of which were signed by 253 signers..

2.2 Preprocessing

An ordinary scanner with normal resolution can be used as an image acquisition device. Scanning hardware may however introduce noise to a signature image. Another source of noise may be speckled paper background on which the signature is signed. Noise on a signature image may have an effect on the feature extraction process and thus experimental results. As such, noise needs reducing or eliminating, if possible.

Signatures are signed with the characteristics of the owners. In many cases, a dot in signatures contains information of authentic signatures. Moreover, other traces of authentic signatures, such as comma and dots, could provide meaningful information to researchers; therefore, such traces are taken into account for off-line signature verification. In order to retain this information, we only eliminate pepper and salt noise for preprocessing. Thus, preprocessing methods should be carefully selected because if a unsuitable process were selected, the information from the main signature could be lost. In this thesis, we have chosen the preprocessing method in which we can eliminate pepper and salt noise to enhance the quality of off-line signature images and the performances of our method.

Normally, off-line signature images consist of three components: main part of the signatures, noise, and image background. With emphasis on eliminating pepper and salt noise, the gray level of each image is adjusted to detect this type of noise. A threshold of gray level is then applied to separate the main part of each signature from the noise part. From original images, we detect the gray level and define the threshold by

$$I_g = round\left(round\left(\sum_{i=1}^{N} \sum_{j=1}^{M} \frac{I_o * s}{G} \right) * \frac{G}{s} \right), \tag{2.1}$$

where I_g refers to grey level image, I_o indicates original image, $and\ N, M$ are two dimensions of original images, $s = 3$ is threshold and G is gray level of original image. If $s = 1\ or\ s = 2$, the

original images will lose much information. The $round$ function in the equation (2.1) is to guarantee that the argument of the function is integer.

Based on this gray level image, a binary mask with the condition below is established:

$$If\ I_g = 255\ then\ I_{bw} = 255\ else\ I_{bw} = 0, \tag{2.2}$$

In the above equation, I_{bw} is a binary image.

And the binary mask is used to cover the main part of original images by the following condition:

$$If\ I_{bw} = 255\ then\ I_{op} = 255\ else\ I_{op} = I_o \tag{2.3}$$

I_{op} is the off-line signature obtained from preprocessing. An example of our preprocessing process is shown in Figure 2.1.

a) b) c) d)

Figure 2.1 Preprocessing; a) Original image; b) Gray level change image; c) Binary image; d) Image after preprocessing.

Figure 2.1 is used to present our preprocessing. It begins from the original image a), from which the gray level change image to detect and eliminate pepper and salt noise is generated b). Binary image is produced in c) to capture the main part of the original image a), and in d) all the pepper and salt noises were eliminate from the original image. This preprocessing has been applied to all signatures in our database.

This chapter has presented the data acquisition process like how database was obtained and stored. This is also the starting phase of our entire off-line signature verification. This phase is aimed for preparing better quality images and improving performance of our work as well.

Chapter 3

Feature Extraction

3.1 Texture recognition

Human eyes are able to recognize the similarities and differences of two different textures, but this very same task poses a great challenge to the machines. However, texture analysis plays an important and useful part in machine vision, such as practical vision machines have to able to handle with textured world surrounding it, image processing. Texture analysis has been applied in a variety of applications. In mature domains, texture analysis plays a major role in, for example, automated inspection, medical image processing, document processing, and remote sensing. In such applications, the learning process will be the preparation process for machine information to recognize an object.

There are three common ways of analyzing texture

Statistical approach is an obvious way to describe such textures is via their statistical properties.

Structural approach is the basic scheme is to build a grammar for the texture and then parse the texture to see it matches the grammar. The idea can be extended by defining texture primitives; simple patterns from which one is more complicated ones can be built. The parse tree for the pattern in a particular region can be used as a descriptor.

Spectral approach is in the frequency domain. If textures are periodic patterns, does it make sense to analyze them with periodic functions? The entire frequency domain is as much as information as the image itself. We can condense the information by collapsing a particular frequency across all orientations or by collapsing all frequencies in a particular orientation.

There are three main ways that textures are used

To discriminate between different regions or to classify them (1)

To produce descriptions so that we can reproduce textures (2)

To segment an image based on textures (3)

For the off-line signature verification purpose, we mainly focus on the first case of the texture analysis in which we extract the texture features by using methods like GLCM, Gabor filters, Local phase quantization. We have stared with the basic information extraction of texture analysis like gray level change during the main part of texture to the famous texture analysis methods like gray level co-occurrence matrix, Gabor filter and the new one is local phase quantization(LPQ).

3.2 Gray level co-occurrence matrix (GLCM)

3.2.1 GLCM background

The work of (R.M Haralick, 1973) first introduces the use of co-occurrence matrix probabilities using GLCM or spatial gray level co-occurrence matrices for extracting various texture features. GLCM is "A two dimensional histogram of gray levels for a pair of pixels, which are separated by a pixel spatial relationship". The GxG gray level co-occurrence matrix P_d for a displacement vector $d = (dx, dy)$ is defined as follows.

The entry (i, j) of P_d is the number of occurrence of the pair of gray levels i and j which are a distance d apart. Formally, it is given as

$$P_d = |\{((r,s),(t,v)) : I(r,s) = i, I(t,v) = j\}| \quad (3.1)$$

where $(r,s),(t,v) \in NxN$, $d = (t,v) = (r + dx, s + dy)$ and $|.|$ is the cardinality of a set. GLCM of an image is computed using displacement vector d, defined by its radius r and orientation θ. A 4x4 image is presented Table 3.1 with gray-stone values equal to 3. A generalized GLCM for that image is shown in Table 3.2, where #(i,j) stands for the number of times gray stone i and j are the neighbors satisfying the condition stated by displacement vector d.

Table 3.1 Test Image

0	0	1	1
0	0	1	1
0	2	2	2
2	2	3	3

Table 3.2 GLCM general form

Gray Tone	0	1	2	3
0	#(0,0)	#(0,1)	#(0,2)	#(0,3)
1	#(1,0)	#(1,1)	#(1,2)	#(1,3)
2	#(2,0)	#(2,1)	#(2,2)	#(2,3)
3	#(3,0)	#(3,1)	#(3,2)	#(3.3)

The four GLCM's for angles of 0^o, 45^o, 90^o, 135^o with the radius of 1 are shown below:

Table 3.3 GLCM for $\theta = 0^o$

4	2	1	0
2	4	0	0
1	0	6	1
0	0	1	2

Table 3.4 GLCM for $\theta = 45$ degrees

4	1	0	0
1	2	2	0
0	2	4	1
0	0	1	0

Table 3.5 GLCM for $\theta = 90$ degrees

6	0	2	0
0	4	2	0
2	2	2	2
0	0	2	0

Table 3.6 GLCM for $\theta = 135$ degrees

2	1	0	0
1	2	1	0
3	1	0	2
0	0	2	0

Frequency normalization can be employed by dividing value in each cell by the total number of possible pixel pair. The GLCM suffers from a number of difficulties like no well-established way to select the displacement vector d and compute co-occurrence matrices for different values of is not always feasible. However, there are several advices for displacement vector d selection and orientation θ selection.

GLCM is related to statistical analysis which needs the computation of texture feature from statistical distribution of observed combination of intensities at specified positions relative to each other in an image. The characteristics of intensity points in each combination are spotted which leads to the classification of texture statistics as first-order, second-order, or higher order. Therefore, working on texture analysis or particularly in GLCM can unveil the information of ink distribution which tells us about personal behavior of signers, pen writing, pressure and speed.

Working with GLCM, researchers have to face with various choices of GLCM radius, GLCM orientations, and a compatible gray level of image to apply GLCM. Thus, the following parts of this section will discuss in greater detail these issues.

3.2.1.1 The choice of GLCM radius

Various research studies show radius r values ranging from 1 to 10. Applying large displacement value to a fine texture would yield a GLCM that does not capture detailed textural information. From these studies, it has been concluded that overall classification accuracies with $r = 1, 2, 4, 8$ are acceptable with the best results for $r = 1$ and $r = 2$. This conclusion is justified as a pixel is more likely to be correlated to other closely located pixel than the one located far away.

3.2.1.2 The choice of GLCM orientations

Every pixel has eight neighboring pixels allowing eight choices for θ , which are $0^o, 45^o, 90^o, 135^o, 180^o, 225^o, 270^o, 315^o$. However, with consideration of the definition of GLCM, the co-occurrence pairs obtained by choosing 0^o would be similar to those obtained by choosing θ equal to $180^o, 225^o, 270^o,$ and 315^o. Therefore, four directions are used to calculate GLCM and its features.

3.2.1.3 The choice of gray level (G)

The dimension of a GLCM is determined by maximum gray level of the pixel. The number of gray levels is an important factor in GLCM computation. More levels would mean more accurate extracted texture information, with increased computational costs. The computational complexity of GLCM method is highly sensitive to the number of gray levels and is proportional of $O(G^2)$.

Therefore, GLCM requires a pairs of r, θ and the value of gray G. Various GLCM parameters are related to specific first order statistical concepts. For example, contrast would mean pixel pair repetition rate, variance would mean spatial frequency detection. The association of these parameters on texture is very critical. The GLCM dimension relates to gray level of original images and stores the co-occurrence probabilities. Texture features are based on statistics which summarize the relative frequency distribution which in turn describes how often one gray tone will appear in a specified spatial relationship to another gray tone on the image.

3.2.2 GLCM texture features

The work of (R.M Haralick, 1973) proposed a number of useful texture features that can be computed from the GLCM. To define these features, several notations are used as follows

$g^{ij} = (i,j)^{th}$ entry in GLCM

$g_x(i) = i^{th}$ entry in marginal probability matrix

$$g_{ij} = \sum_{j=1}^{N_g} g(i,j)$$

N_g = Number of distinct gray levels in the image

$$\sum_{i} = \sum_{i=1}^{N_g}$$

$$\sum_{j} = \sum_{j=1}^{N_g}$$

$$g_y(i) = \sum_{i=1}^{N_g} g(i,j)$$

$g_{x+y}(k) = \sum_{i=1}^{N_g} \sum_{j=1}^{N_g} g(i,j)$ where $i + j = k = 2,3,\ldots,2N_g$

$g_{x-y}(k) = \sum_{i=1}^{N_g} \sum_{j=1}^{N_g} g(i,j)$ where $|i - j| = k = 0,1,2\ldots,N_g - 1$

GLCM Energy Feature

$$f_1 = \sum_{i} \sum_{j} g_{i,j}^2 \tag{3.2}$$

GLCM Entropy Feature

$$f_2 = -\sum_{i} \sum_{j} g_{ij} log_2 g_{ij} \tag{3.3}$$

GLCM Contrast Feature

$$f_3 = \sum_{i} \sum_{j} (i-j)^2 g_{ij} \tag{3.4}$$

GLCM Variance Feature

$$f_4 = \sum_{i} \sum_{j} (i-\mu)^2 g_{ij} \tag{3.5}$$

where μ is mean of g_{ij}

GLCM Homogeneity Feature

$$f_5 = \sum_{i} \sum_{j} \frac{1}{1+(i-j)^2} g_{ij} \tag{3.6}$$

GLCM Correlation Feature

$$f_6 = \frac{\sum_i \sum_j (ij) g_{ij} - \mu_x \mu_y}{\sigma_x \sigma_y} \quad (3.7)$$

where $\mu_x, \mu_y, \sigma_x, \sigma_y$ are means and standard deviations of g_x and g_y

GLCM Sum Average Feature

$$f_7 = \sum_{i=2}^{N_g} i g_{x+y}(i) \quad (3.8)$$

GLCM Sum Entropy Feature

$$f_8 = -\sum_{i=2}^{2N_g} g_{x+y}(i) \log\{g_{x+y}(i)\} \quad (3.9)$$

GLCM Sum Variance Feature

$$f_9 = \sum_{i=2}^{2N_g} (i - f_7)^2 \, g_{x+y}(i) \quad (3.10)$$

GLCM Difference Variance Feature

$$f_{10} = Variance\ of\ g_{x-y} \quad (3.11)$$

GLCM Difference Entropy Feature

$$f_{11} = -\sum_{i=0}^{N_g - 1} g_{x-y}(i)\, log\{g_{x-y}(i)\} \quad (3.12)$$

GLCM Dissimilarity Feature

$$f_{12} = \sum_i \sum_j P_{ij} |i - j|, \quad (3.13)$$

GLCM texture features present exactly human perception point of view on a texture. Therefore, each GLCM feature carries with its physical meaning as listed bellow

Energy is also called Uniformity or Angular second moment, measures the texture uniformity that is pixel pair repetitions. It detects disorders in textures and reaches a maximum value equal to one. High energy values occur when the gray level distributions has constant or periodic form. Energy has a normalized range; the GLCM of less homogeneous image will have large number of small entries.

Entropy measures the disorder or complexity of an image. The entropy is large when the image is not texturally uniform and many GLCM elements have very small values. Complex textures tend to have high entropy. Entropy is strong but inversely correlated to energy.

Contrast measures the spatial frequency of an image and its difference moment of GLCM. It is the difference between the highest and the lowest values of a contiguous set of pixels. It measures the amount of local variations present in the image. A low contrast image presents GLCM concentration term around the principal diagonal and features low spatial frequencies.

Variance measures the heterogeneity and strongly relates to the first order statistical variable such as standard deviation. Variance increases when the gray level values differ from their mean.

Homogeneity or Inverse Difference Moment measure homogeneity as it assumes larger values for smaller gray tone difference in pair elements. It is more sensitive to the existence of near diagonal elements in the GLCM. It has maximum value when all elements in the image are identical. GLCM contrast and homogeneity are strongly, but inversely, correlated in terms of equivalent distribution in pixel pairs population. It means homogeneity decreases if contrast increases while energy is kept constant.

The correlation feature is a measure of gray stone linear dependencies in the image.

The texture features described above like angular second moment, entropy, sum entropy, difference entropy, information measure of correlation and the maximal correlation features are GLCM features that related to the invariance property. Work of (Z. Wang, 2002) reported that "Energy" and "Contrast" are the most efficient parameters for discriminating different texture patterns. The general thumb rules used in the selection of texture features can be stated as follows:

Energy is preferred to entropy as its values belong to normalized range

Contrast is associated with the average gray level difference between neighborhood pixels. It is similar to variance; however preferred, due to its reduced computational load and effectiveness as a spatial frequency measure.

Energy and Contrast are the most significant parameters in terms of visual assessment and computational load to discriminate between different texture patterns.

3.2.3 GLCM application for texture analysis

GLCM has been widely used in field of image processing and applied for variety applications from texture analysis related to gray scale and color texture recognition. Work of (L. Soh, 1999) used GLCM to quantitatively evaluate textural parameters and to determine which parameter values and representations are the best for mapping sea ice texture. The work of (M. M. Mokji, 2007) applied both Haar wavelet transform and GLCM and the Haar wavelet bands had related to orientation elements in GLCM computation. Their work also reduced GLCM computation using Haar wavelet.

3.3 Gabor filter

3.3.1 Gabor filter background

Gabor filter was published by Dennis Gabor in 1946 when he proposed the use of special elementary function to present signals in time and frequency simultaneously (Gabor, 1946).Having modeled the spatial summation properties of the receptive fields in the primary visual cortex, Gabor filters are very popular in various image processing applications.

A 2D Gabor function is formed by the product of a 2D Gaussian and a complex exponential function. Gabor function acts as low-level, oriented edge and texture discriminators that are sensitive to different frequencies and scale information. In an informational theoretical sense, Gabor[38] had discovered that Gaussian-modulated complex exponentials provides the best trade-off between spatial and frequency resolution, allowing simultaneously good spatial localization and description of signal structures. Other interesting properties of Gabor response are the invariance to change in image contrast and robustness with respect to small translations of the image pattern in consideration.

Gabor filters consist of the product between an elliptical Gaussian and a sinusoidal. It can be assumed for simplicity that the rotations of the Gaussian and the sinusoidal are the same, i.e. their principal axes correspond to the x and y axes. Figure 1.3 shows a visual combination between Gaussian and sinusoid to form Gabor filters.

Gabor filters have been widely used in numerous applications such as texture recognition (J. Y. Tou), finger print and palm print segmentation (H B Kre, 2009) and signature verification (H B Kekre, 2010).

Common to all Gabor features is that they are based on Gabor filter response for a given input image. The responses all over the image are calculated for a set of filters, a bank. These filters will be tuned to various orientations and frequencies.

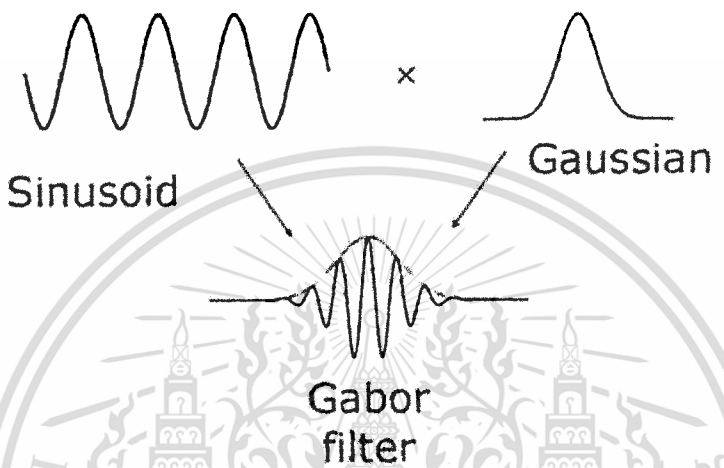

Figure 3.1 Visual presentation of the Gabor filter (Berisha S. , 2009).

3.3.2 Gabor filters

The definition of Gabor filters is presented below.

1-D Gabor elementary function can be defined as the product of the pulse of a probability function with a harmonic oscillation of any frequency:

$$g(t) = e^{-\alpha^2(t-t_o)^2} e^{i2\pi f_o t+\varphi} \tag{3.14}$$

where α is the time duration and bandwidth of the Gaussian envelope, t_o denotes its centroid, f_o is the frequency of sinusoidal or carrier and φ denotes phase shift. The 1-D Fourier transform of the above Gabor element function is

$$G(f) = \sqrt{\frac{\pi}{\alpha^2}} e^{-(\frac{\pi}{\alpha})^2(f-f_o)^2} e^{-i2\pi(f-f_o)t+\varphi} \tag{3.15}$$

The Gabor elementary function in (3.14) is concentrated near the time instant t_o and thus convolution of the origin-center filter is preferred, we set $t_o = 0$ and $\varphi = 0$. Therefore, we consider Gabor elementary functions of the form as bellow

$$g(t) = e^{-\alpha^2 t^2} e^{i2\pi f_o t} \tag{3.16}$$

These functions are the most complicated linear filters. Therefore, the calculation of the 1-D filter response of a function ξ at home location t_1 with convolution is shown as follows

$$\begin{aligned} r(t_1) &= g(t_1) \otimes \xi(t_1) \\ &= \int g(t_1 - t)\, \xi(t) dt \\ &= \int e^{-\alpha^2 (t_1 - t)^2} e^{j2\pi f_o (t_1 - t)} \xi(t) dt \\ &= e^{j2\pi f_o t_1} \int e^{-\alpha^2 (t_1 - t)^2} e^{-j2\pi f_o t} \xi(t)\, dt \end{aligned} \tag{3.17}$$

Several problems emerge when applying Gabor filter to certain applications; for example, lack of control α, the time duration and bandwidth of the filter. Several works have solved these issues by several methods like in (Berisha, 2009). They approached from multi-resolution analysis and wavelets to guarantee that the filters on different frequencies are scaled version of each other;

The time duration of the filter is connected to the central as follows

$$\alpha = \frac{|f_o|}{\gamma}, \tag{3.18}$$

where f_o is the central frequency of the filter and the γ controls the effective width of the filter (Berisha, 2009). Substituting (3.18) for α into equation (3.16), the following is obtained:

$$g(t) = e^{-\left(\frac{|f_o|}{\gamma}\right)^2 t^2} e^{j2\pi f_o t} \tag{3.19}$$

From equation (3.15), the peak filter response occurs at $f = f_o$, and $max_f\big(G(f)\big) = \sqrt{\frac{\pi}{\alpha^2}}$. Thus, $\sqrt{\frac{\alpha^2}{\pi}}$ can be used as normalization factor in the definition of Gabor filters. Then the normalized 1-D Gabor filter function is defined as

$$g(t) = \sqrt{\frac{\alpha^2}{\pi}} e^{-(\frac{|f_o|}{\gamma})^2 t^2} e^{j2\pi f_o t} = \frac{|f_o|}{\gamma\sqrt{\pi}} e^{-(\frac{|f_o|}{\gamma})^2 t^2} e^{i2\pi f_o t} \tag{3.20}$$

The Fourier domain $g(t)$ is determined by

$$G(f) = e^{-\frac{\gamma\pi}{f_0}(f-f_0)^2} \tag{3.21}$$

3.3.3 Two dimensional Gabor filters

The 1-D Gabor filter in equation (3.20) can be developed into two dimensions. In this version, the 2-D Gabor filters replace t by spatial coordinates (x, y) in the space domain. Frequency variables (u, v) are used instead of frequency variable f. Image processing is the main reason that leads to 2-D version of Gabor filters were exploited. The typical form of 2-D Gabor function is defined as following in spatial domain

$$g(x,y) = \mathrm{g(x,y;}f_0, \theta) = \exp\{-\frac{1}{2}[\frac{{x_\theta}^2}{{\sigma_x}^2} + \frac{{y_\theta}^2}{{\sigma_y}^2}]\cos(2\pi f x_\theta)\} \tag{3.22}$$

where $x_\theta = xcos\theta + ysin\theta, y_\theta = -xsin\theta + ycos\theta$, and θ is the rotation angle of the Gaussian major axes and the plane wave (sinusoidal). $\theta_k = \frac{\pi(k-1)}{m}, k = 1, \ldots, m$ and m is the numbers of orientations.

With the aim for guaranteeing that filters in different frequencies are scaled versions of each other as the 1-D case, the substitution of $\alpha = \frac{|f_0|}{\gamma}$ and $\beta = \frac{|f_0|}{\eta}$. Now γ and η control the bandwidth of the filter along x and y axes. The normalized compact near form of the 2-D Gabor filter function is expressed as

$$g(x,y) = \frac{f_o^2}{\pi\gamma\eta} e^{-(\frac{f_o^2}{\gamma^2}x_p^2 + \frac{f_o^2}{\eta^2}y_p^2)} e^{j2\pi f_o x_p}$$

The 2-D filter given in equation (3.22) represents a group of wavelets which optimally captures both local orientation and frequency information from images. Each off-line signature image is filtered with $G(x, y)$ at various orientations, frequencies and standard deviations. Therefore, the applications of Gabor filters for off-line signature images need an appropriate selection of filter parameters. An appropriately designed filter will extract useful information such as spots and edges. For example, based on pixels with large magnitudes in the particulars filter response, one can determine the presence of strong edges of certain orientation in different images. Filters can be performed at different scales to find patterns of different sizes. In addition, 2-D Gabor filters provide some of the benefits of Fourier

analysis, which preserve spatio-frequency locality, thus allowing the study of the spatial distribution of texture. They enable detection of gradual changes of texture and texture variations (Berisha, 2009).

3.3.4 Basic Gabor feature space

Different Gabor filter parameters can be used to extract different features. The frequency and orientation of the Gabor filters are some of the most useful parameters. In order to distinguish between objects in most cases it is necessary to apply several Gabor filters to an image by forming a so called "filter bank" and then for classification purposes we can look at the relationship between Gabor responses of different images. The selection of discrete rotation angles θ_k is very important, and it has been shown that the orientations must be spaced uniformly as

$$\theta_k = \frac{k2\pi}{n} \tag{3.23}$$

for $k = 0, \dots, n-1$ where k_{th} is orientation and n is the number of orientations to be used. A Gabor filter matrix is defined to visualize how Gabor filter works with its orientation like bellow

$$G = \begin{bmatrix} g(x_o, y_o; f_o, \theta_o) & g(x_o, y_o; f_o, \theta_1) & \dots & g(x_o, y_o; f_o, \theta_{n-1}) \\ g(x_o, y_o; f_1, \theta_o) & g(x_o, y_o; f_1, \theta_1) & \dots & g(x_o, y_o; f_1, \theta_{n-1}) \\ \dots & \dots & \dots & \dots \\ g(x_o, y_o; f_{m-1}, \theta_o) & g(x_o, y_o; f_{m-1}, \theta_1) & \dots & g(x_o, y_o; f_{m-1}, \theta_{n-1}) \end{bmatrix} \tag{3.24}$$

where each element $g(x_o, y_o; f_1, \theta_o)$ presents the Gabor filter response at location (x_o, y_o), f_i and θ_i are sample parameters in equation(3.20), and for $i = 0, \dots, m-1$ and $j = 0, \dots, n-1$.

3.4 Local phase quantization

3.4.1 Local phase quantization overview

The local phase quantization (LPQ) operator was originally proposed by Ojansivu and Heikkila as texture descriptor (V. Ojansivu J. H., 2008). LPQ is based on the blur invariance property of the Fourier phase spectrum. It uses the local phase information extracted using the 2-D short term Fourier transform (STFT) computed over a rectangular neighborhood at each pixel position of the image. In LPQ only four complex coefficients are considered, corresponding to 2-D frequencies.

Although LPQ is originally created for blur texture classification, it is still practical for other textures. The code produced by the LPQ operator is insensitive to centrally symmetric blur which includes

motion, out of focus and atmosphere turbulence blur. The LPQ operator is applied to texture identification by computing it locally at every pixel location and presenting the result codes as a histogram. Local frequency analysis, often referred to signal processing methods, has also been used for texture analysis previously.

In image processing, the discrete model for spatial invariant blurring of an original image $f(\boldsymbol{x})$ resulting in an observed image $g(\boldsymbol{x})$ can be expressed by a convolution, given by

$$g(\boldsymbol{x}) = (f * h)(\boldsymbol{x}), \tag{3.25}$$

where $h(\boldsymbol{x})$ is the point spread function (PSF) of the blur, *denotes 2-D convolution and $\boldsymbol{x}$ is a vector of coordinates $[x, y]^T$. In the Fourier domain, this corresponds to

$$G(\boldsymbol{u}) = F(\boldsymbol{u}).H(\boldsymbol{u}), \tag{3.26}$$

Where $G(\boldsymbol{u}), F(\boldsymbol{u})$ and $H(\boldsymbol{u})$ are the discrete Fourier transforms (DFT) of the texture image $g(\boldsymbol{x})$, and the point spread function $h(\boldsymbol{x})$, respectively and $\boldsymbol{u}$ is a vector of coordinates $[u, v]^T$. We may separate the magnitude and phase parts of (3.26), resulting in

$$\begin{aligned} |G(\boldsymbol{u})| &= |F(\boldsymbol{u})|.|H(\boldsymbol{u})|, \\ \angle G(\boldsymbol{u}) &= \angle F(\boldsymbol{u}) + \angle H(\boldsymbol{u}), \end{aligned} \tag{3.27}$$

If we assume that the $h(\boldsymbol{x})$ is centrally symmetric, i.e. $h(\boldsymbol{x}) = h(-\boldsymbol{x})$, its Fourier transform is always real-valued, and as a consequence its phase is only a two-value function, given by

$$\angle H(\boldsymbol{u}) = \begin{cases} 0 & if\ H(\boldsymbol{u}) \geq 0 \\ \pi & if\ H(\boldsymbol{u}) < 0' \end{cases} \tag{3.28}$$

This means that

$$\angle G(\boldsymbol{u}) = \angle F(\boldsymbol{u}) \text{ for all } H(\boldsymbol{u}) \geq 0 \tag{3.29}$$

In other words, the phase of observed image $\angle G(\boldsymbol{u})$ at the frequencies, where $H(\boldsymbol{u})$ is positive, is invariant to centrally symmetric blur.

The local phase quantization (LPQ) method is based on the blur invariance property of the Fourier phase spectrum. It uses the local phase information extracted using the 2-D DFT or short term Fourier

transform (STFT) computed over a rectangular $M - by - M$ neighborhood $\aleph_x$ at each position $\boldsymbol{x}$ of the image $f(\boldsymbol{x})$ define by

$$F(\boldsymbol{u}, \boldsymbol{x}) = \sum_{y \in \aleph_x} f(\boldsymbol{x} - \boldsymbol{y})\, e^{-j2\pi \boldsymbol{u}^T \boldsymbol{y}} = \boldsymbol{w_u}^T \boldsymbol{f_x} \tag{3.30}$$

where $\boldsymbol{w_u}$ is the basis vector of the 2-D DFT at frequency $\boldsymbol{u}$, and $\boldsymbol{f_x}$ is another vector containing all M^2 image sample from $\aleph_x$.

As it can be previously noticed, an efficient way of implementing the STFT is the use 2-D convolutions $f(\boldsymbol{x}) * e^{-2\pi j \boldsymbol{u}^T \boldsymbol{x}}$ for all $\boldsymbol{u}$. Since the basic functions are separable, computation can be performed using 1-D convolutions for the rows and columns.

In LPQ only four complex coefficients are considered, corresponding to 2-D frequencies $\boldsymbol{u_1} = [a, 0]^T, \boldsymbol{u_2} = [0, a]^T, \boldsymbol{u_3} = [a, a]^T$ *and* $\boldsymbol{u_4} = [a, -a]^T$ where a is a scalar frequency below the first zero crossing of $H(\boldsymbol{u})$ that satisfies the condition (3.29). Let

$$\boldsymbol{F_x}^c = [F(\boldsymbol{u_1}, \boldsymbol{x}), F(\boldsymbol{u_2}, \boldsymbol{x}), F(\boldsymbol{u_3}, \boldsymbol{x}), F(\boldsymbol{u_4}, \boldsymbol{x})] \tag{3.31}$$

$$\boldsymbol{F_x} = [Re\{\boldsymbol{F_x}^c\}, Im\{\boldsymbol{F_x}^c\}] \tag{3.32}$$

where Re{.} and Im{.} are return real and imaginary parts of a complex number, respectively. Let us assume that image function $f(\boldsymbol{x})$ is the result of a first order Markov process, where the correlation coefficient between adjacent pixel values is ρ and the variance of each sample is σ^2. Without a lost of generality we can assume that $\sigma^2 = 1$. As a result, the covariance between positions $\boldsymbol{x_i}$ and $\boldsymbol{x_j}$ becomes

$$\sigma_{ij} = \rho^{||\boldsymbol{x_i} - \boldsymbol{x_j}||}, \tag{3.33}$$

where $||.||$ denotes norm and the covariance matrix of all M samples in $\aleph_x$.

$$\boldsymbol{C} = \begin{bmatrix} 1 & \sigma_{12} & \cdots & \sigma_{1M} \\ \sigma_{21} & 1 & \cdots & \sigma_{2M} \\ \vdots & \vdots & \ddots & \vdots \\ \sigma_{M1} & \sigma_{M2} & \cdots & 1 \end{bmatrix} \tag{3.34}$$

Hence, the covariance matrix of the transform coefficient vector $F(\boldsymbol{x})$ can be obtained from

$$\boldsymbol{D} = \boldsymbol{WCW}^T, \tag{3.35}$$

One can easily notice that $\boldsymbol{D}$ is not a diagonal matrix for $\rho > 0$ meaning that the coefficients are correlating.

Before quantization the coefficients are decorrelated, because it can be shown that the information is maximally preserved in scalar quantization, quantized samples are statistically independent. Assuming Gaussian distribution, independence can be achieved using a whitening transform

$$\boldsymbol{G_x} = \boldsymbol{V}^T \boldsymbol{F_x}, \tag{3.36}$$

where $\boldsymbol{V}$ is an orthonormal matrix derived from the singular value decomposition (SVD) of the matrix $\boldsymbol{D}$ that is

$$\boldsymbol{D} = \boldsymbol{D\Sigma V}^T, \tag{3.37}$$

Notice that $\boldsymbol{V}$ can be solved in advance for a fixed value of ρ. Next, $\boldsymbol{G_x}$ is computed for all image positions, i.e. $\boldsymbol{x} \in \{\boldsymbol{x_1}, \boldsymbol{x_2}, \dots, \boldsymbol{x_N}\}$ and the resulting vectors are quantized using a simple scalar quantizer.

$$q_i = \begin{cases} 1, & if\ g_i \geq 0 \\ 0, & otherwise \end{cases} \tag{3.38}$$

where g_i is the jth component of $\boldsymbol{G_x}$. The quantized coefficients are represented as integer values between 0-255 using binary coding

$$b = \sum_{j=1}^{8} q_j 2^{j-1} \tag{3.39}$$

Finally, a histogram of these integer values from all image positions is composed and used as a 256-dimensional feature vector in classification.

The resulting integers b are invariant to centrally symmetric texture provided that the window $\aleph_x$ is infinitely large and the frequency spectrum of the blur PSF is positive at the sample locations $\boldsymbol{u_1} - \boldsymbol{u_4}$. The second condition is easily met if a is sufficiently small. However, the first condition cannot be fulfilled by practice therefore, complete invariance is not achieved but a relatively small scalar is enough for the robustness.

3.4.2 LPQ applications

One can easily notice that $\boldsymbol{D}$ is not a diagonal matrix for $\rho > 0$ meaning that the coefficients are correlating.

Before quantization the coefficients are decorrelated, because it can be shown that the information is maximally preserved in scalar quantization, quantized samples are statistically independent. Assuming Gaussian distribution, independence can be achieved using a whitening transform

$$\boldsymbol{G_x} = \boldsymbol{V}^T \boldsymbol{F_x}, \tag{3.36}$$

where $\boldsymbol{V}$ is an orthonormal matrix derived from the singular value decomposition (SVD) of the matrix $\boldsymbol{D}$ that is

$$\boldsymbol{D} = \boldsymbol{D\Sigma V}^T, \tag{3.37}$$

Notice that $\boldsymbol{V}$ can be solved in advance for a fixed value of ρ. Next, $\boldsymbol{G_x}$ is computed for all image positions, i.e. $\boldsymbol{x} \in \{\boldsymbol{x}_1, \boldsymbol{x}_2, \ldots, \boldsymbol{x}_N\}$ and the resulting vectors are quantized using a simple scalar quantizer.

$$q_i = \begin{cases} 1, & if\ g_i \geq 0 \\ 0, & otherwise \end{cases} \tag{3.38}$$

where g_i is the jth component of $\boldsymbol{G_x}$. The quantized coefficients are represented as integer values between 0-255 using binary coding

$$b = \sum_{j=1}^{8} q_j 2^{j-1} \tag{3.39}$$

Finally, a histogram of these integer values from all image positions is composed and used as a 256-dimensional feature vector in classification.

The resulting integers b are invariant to centrally symmetric texture provided that the window $\aleph_x$ is infinitely large and the frequency spectrum of the blur PSF is positive at the sample locations $\boldsymbol{u}_1 - \boldsymbol{u}_4$. The second condition is easily met if a is sufficiently small. However, the first condition cannot be fulfilled by practice therefore, complete invariance is not achieved but a relatively small scalar is enough for the robustness.

3.4.2 LPQ applications

The work of (V. Ojansivu E. R., 2008) applied LPQ for blur insensitive texture analysis. They estimated the local characteristic orientation, and the second step was then to extracts a binary descriptor vector. Both steps of the algorithm apply the phase of the locally computed Fourier transform coefficients which can be shown to be insensitive to centrally symmetric image blurring. (S. Brahnam L. N.-Y., 2010)'s work applied techniques that combine an indirect descriptor with a direct representation using local phase quantization.

3.5 Feature vector extraction

We have applied several methods to extract features of off-line signatures to verify the genuine and forged signatures. In this thesis, four methods have been studied to determine the most effective one for off-line signature verification. After feature extraction process, we will generate feature vectors to classify genuine and forged signatures; bellows are our study presentations via methods that have been conducted to off-line signature texture.

3.5.1 Off-line signature verification based on FIR system characterizing gray level change of signature image

3.5.1.1 Gray level change

Working in the off-line signature verification environment, researchers face several issues, such as lack of dynamic information of signature image of pen-tip coordinates, pressure, velocity, acceleration, pen up, pen down, which can be captured by tablets. The limited amount of graphical characteristics in off-line signature verification requires a fundamental knowledge of writing and ink deposition. While online method is based on the availability of a one-dimension (1D) vector where elements are pairs of (x, y) coordinates of the pen-tip, the off-line signature verification method is concerned only with the attempts to recognize images of signatures that are signed on papers with no temporal information. Thus, for off-line signature verification method, we observe the change of gray level in each image and then compare the differences between genuine and forged ones to figure out the authentic signatures. There are several questions we have to answer when working on this issue like what the effects on the ink trace on off-line signature image textures? Is there any significant difference between gray level of

forged and genuine signature? What do the gray level changes effect the authentication of signature? From this motivation, we have conducted research about gray level change of the main part of signature, along the border of signature. It is noticed that gray level change method had been applied for off-line signature images in our database which was obtained and reserved to public in a standard condition.

In off-line signature verification, shape of signature is one of the most important features to verify random forged signatures who sign without any information about authentic signatures. However, for skilled forgers who have seen genuine signatures and their forged signatures are almost similar to the genuine ones, merely considering shape of the signature to determine between genuine and forged signatures is not always effective.

In this work, in order to pinpoint the forged signatures, the features related to gray level change of signature images are taken into account. As such, four features are extracted and divided into two groups. In the first group, the features are extracted from the whole signatures, while in the second group we concentrate on the gray level change along the border of each signature.

In the first group, gray level change and histogram features of signature images are detected. To extract gray level features of each signature, each signature is divided into fixed size blocks. The difference between the summations of gray levels of two adjacent blocks of signature image as shown in Figure 3.2 is calculated as follows:

$$b(k) = \sum_{i=1}^{M}\sum_{j=1}^{N} B_k(i,j), \tag{3.40}$$

$$g_i = b(k+1) - b(k), \tag{3.41}$$

where $[M, N]$ is sizes of blocks, k is the index of block and $B_k(i,j)$ is gray level of block k^{th} at the position i, j, respectively. The first feature can be determined by connecting together the feature g_i as vector $\boldsymbol{g}' = [g_1, g_2, g_3, \dots g_n]$, n is the number of blocks.

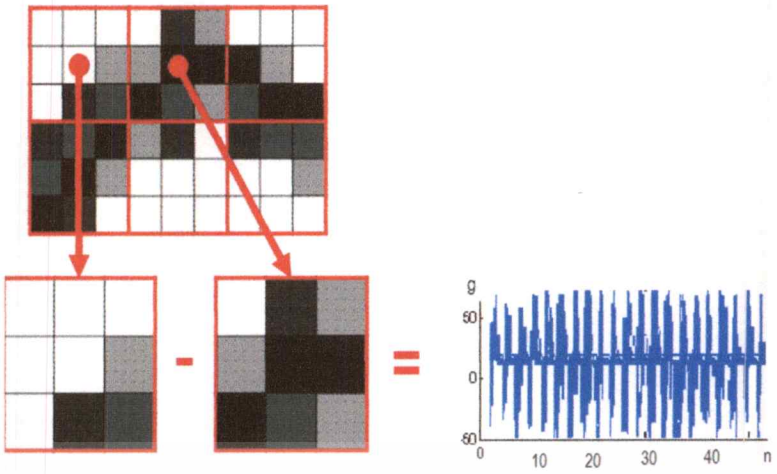

Figure 3.2 Gray level change of off-line signature based on two adjacent blocks.

Figure 3.2 shows the images of gray level change feature extraction of this method. The gray level change in each individual block was calculated and the difference of gray level change between two adjacent blocks was taken into account to form the first feature related to gray level of each signature.

The second feature of gray level of each signature, histogram $t' = [t_1, t_2, \ldots, t_n]$ of off-line signature image is calculated. Figure 3.3 is one example of histogram feature extraction.

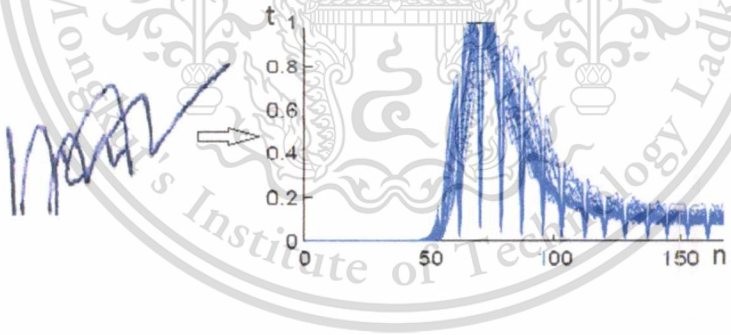

Figure 3.3 Histogram of off-line signature image.

Figure 3.3 shows the histogram feature extraction of the gray level change method. With the meaning of histogram on image texture, this feature will present the influence of histogram on genuine and forged signature images.

In the second group, the gray level change along each signature's borders and its slopes are determined.

For the third feature in group two, the features of handwriting related to gray level change at the border of signatures are extracted. In this case, the borders at the top, left, bottom and right of signature are

detected. The third feature of handwriting is defined as $\boldsymbol{b'} = [b_1, b_2, \ldots, b_n]$ by the combination of gray level at the border of signatures. An example of the third feature is shown in Figure 3.4.

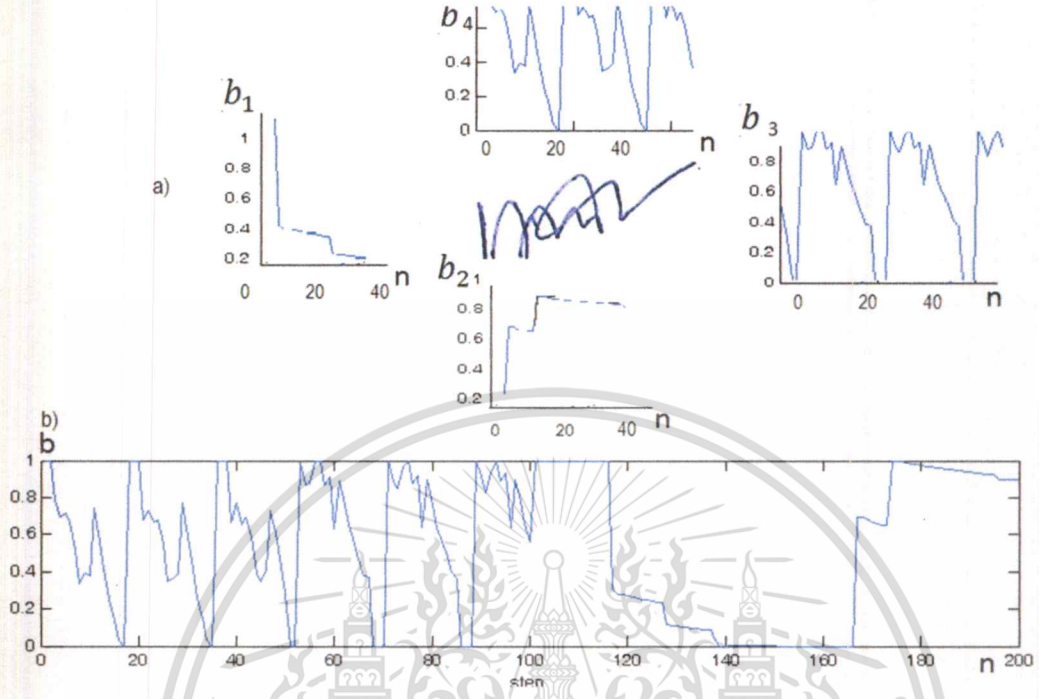

Figure 3.4 Border extraction of off-line signature image; a) off-line signature image with feature extracted from four sides; b) the gray level of four sides presented within one single graph.

Figure 3.4 presents the third feature of gray level change method. In this example, we extracted the gray at the border of one signature. The gray level information of the top, right, bottom, and left of this signature was extracted to form the third feature. This process was repeated for all signatures in our database.

Finally, it can be observed that off-line image signatures signed by different pens are different. In order to extract consistent features of handwriting, the fourth feature of handwriting is determined by calculating slopes of gray level at borders of signature and this feature is stored in $\boldsymbol{s'} = [s_1, s_2, \ldots, s_n]$.

Figure 3.5 shows examples of four features of handwriting obtained from genuine signatures and forgeries for persons A and B in our database. This figure shows original features obtained from gray level change of the main part of each signature, histogram features of each signature, gray level of border signatures, and slope of signatures. Blue features are genuine features, and red feature are

forgery ones. After this step, four features related to gray level of signature were extracted, but fluctuations were generated with these four features. These fluctuations may impact the performances of our methods. Reduction of these fluctuations hence would be discussed in the Discrete Cosine Transform section of this thesis.

3.5.1.2 Discrete cosine transform of the features of the signature images

In order to reduce the fluctuations of features of handwriting, discrete cosine transforms (DCTs) for each feature vector are calculated using equation 3.42 as follows:

$$\Psi_{\varpi} = \sqrt{\frac{2}{M}}\mu(m)\sum_{n=0}^{M-1}\varpi(n)cos[\frac{\pi(2n+1)m}{2M}], \quad (3.42)$$

$$\mu(m) = 1(m \neq 0), \mu(0) = \frac{1}{\sqrt{2}}, \quad (3.43)$$

$$m = 0, 1, 2, \ldots M-1, \varpi = \boldsymbol{g}, \boldsymbol{t}, \boldsymbol{b}, \boldsymbol{s} \quad (3.44)$$

Figure 3.6 shows discrete cosine transform (DCT) features of original features. Compared to previous features, discrete cosine transform features significantly reduced the fluctuations for genuine and forgery features. These discrete cosine transform features would be used as features from genuine and forged signature. Due to the order of discrete cosine transform, we applied various values of order of DCT to determine the influence of the order on genuine and forgery features. However, if the values of order DCT may cause to meaningless part of the features, therefore, the values of DCT order $\boldsymbol{m}$ had been tested in wide range from 15 to 20. This range has been used to experience and figure out the most effective value of order DCT on signature.

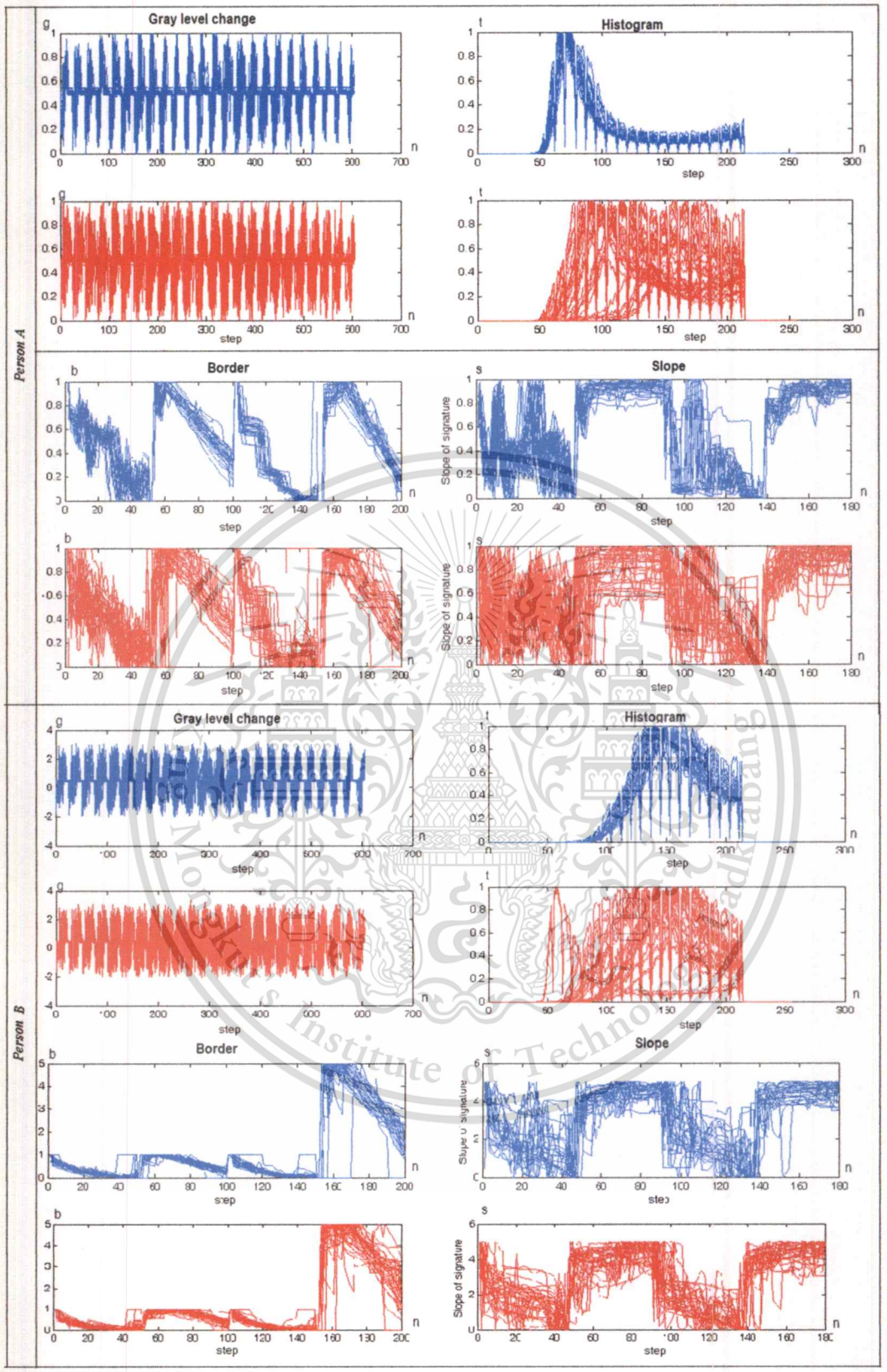

Figure 3.5 Gray level change, histogram, gray level of the border and slope features obtained from person A and person B in our database.

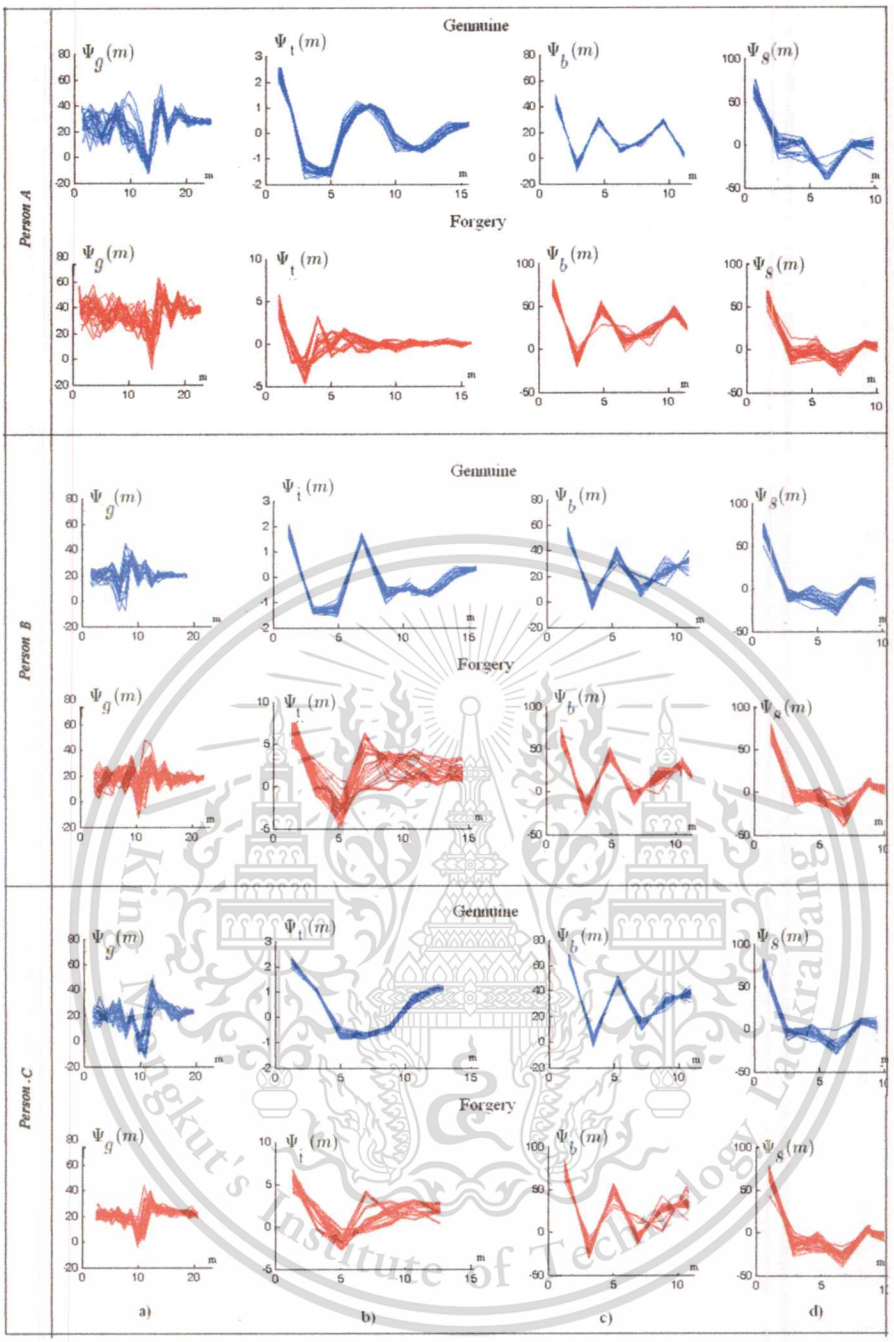

Figure 3.6 Example of discrete cosine transform of gray level change, histogram, gray level of the border and slopes obtained from 3 signers in our database

3.5.1.3 Finite impulse response system characterizing gray level change of signature

In order to characterize the gray level change of the signature, two finite impulse response (FIR) systems are introduced to describe individual features of handwriting. In the first FIR system, Ψ_t and $\hat{\Psi}_g$ are respectively used as input and output of FIR system and in the second FIR system, Ψ_s and $\hat{\Psi}_b$ are used as input and output, where Ψ_t, $\hat{\Psi}_g$, Ψ_s, $\hat{\Psi}_b$ are DCTs of histogram, gray level change of off-

line signatures, slope and gray level of the border of signatures. The two FIR systems mentioned above are presented as follows:

$$\hat{\Psi}_g(k) = \sum_{m=0}^{M} \mathfrak{h}_1(m)\Psi_t(k-m), \tag{3.45}$$

$$\hat{\Psi}_b(k) = \sum_{m=0}^{M} \mathfrak{h}_2(m)\Psi_s(k-m), \tag{3.46}$$

where $\mathfrak{h}_1(m)$ and $\mathfrak{h}_2(m)$ are the impulse responses of two FIR systems, respectively. M is order of the FIR systems. The impulse responses $\mathfrak{h}_1(m)$, $\mathfrak{h}_2(m)$ can be determined by minimizing the least-square error at M as:

$$\mathcal{E}_1 = \sum_{m=0}^{M} [\Psi_t(m) - \hat{\Psi}_g(m)],^2 \tag{3.47}$$

$$\mathcal{E}_2 = \sum_{m=0}^{M} [\Psi_b(m) - \hat{\Psi}_s(m)],^2 \tag{3.48}$$

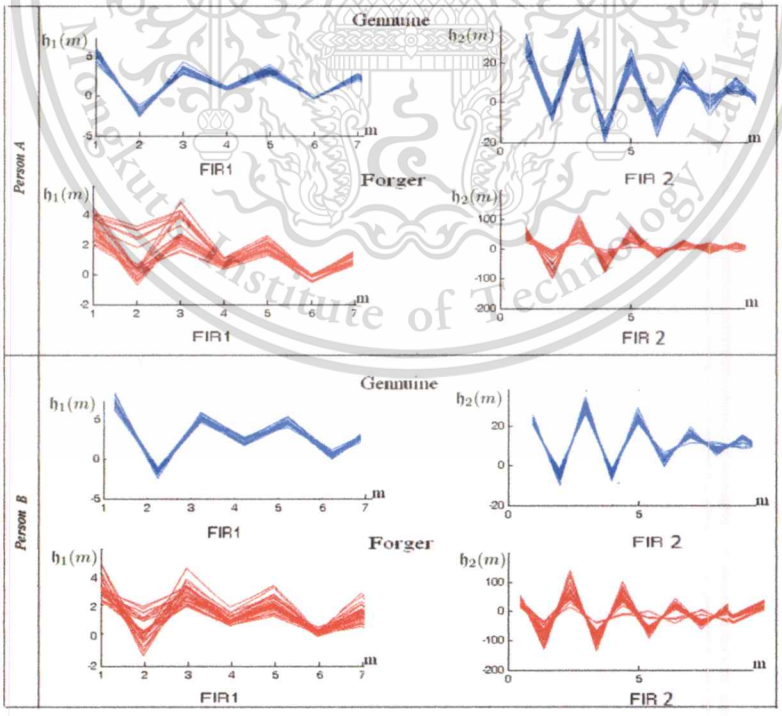

Figure 3.7 Example of impulse responses of the FIR systems obtained from genuine and forgery signatures

The orders of two FIR systems have been ranged from 5 to 10 due to the range of inputs and outputs. Figure 3.7 shows the impulse responses $\mathfrak{h}_1(m), \mathfrak{h}_2(m)$ which are obtained from genuine and forged signatures. It can be seen that the derived impulse responses from genuine signatures are significantly different from those of the forged signatures. Therefore, the impulse responses of the two FIR systems can be used as individual features for off-line signature verification.

3.5.2 Gray level occurrence matrix applied for off-line signature verification

Applying GLCM and its features to off-line signature image, the grey level of image was changed as the rule mentioned in (J. F. Vargas M. F., 2010). In our study, to apply GLCM calculation, the gray level of off-line signature images is changed grey level using the following equation.

$$I_1 = round(\frac{I_{op} * k}{G}) \tag{3.49}$$

where I_{op} is the image obtained from preprocessing step, I_1 is the denotation of image after changing the grey, G is grey level of original image signature before GLCM calculation and k is the selected level to reduce gray level. The gray level of original images was changed to reduce the complexity in the GLCM calculation. Since the original gray levels of off-line signature images will be responsible for the size of GLCM matrices, this leads to the gray level change to optimize the GLCM matrix size. Therefore, in our experiment $k = 7$ is acceptable for image with gray level 8.

Each image texture is calculated by using a set of gray level concurrence matrix (GLCM) for texture analysis, the GLCM calculates the probability at a certain grey level of pixel and the difference in a prescribed direction due to a distance from its neighboring pixels, GLCM formula was presented in equation (3.1). In this thesis, direction θ is determined by vector $[d_x, d_y]$ is presented in four directions $0^0, 45^o, 90^o$ and 135^o from the interest point (i, j) which is shown in Figure 3.8.

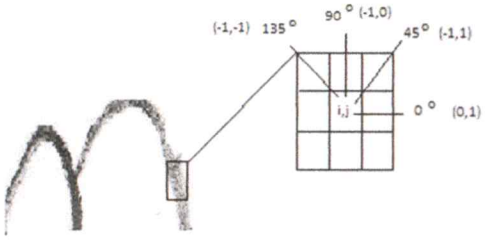

Figure 3.8 Neighboring pixels with four directions

The calculation of GLCM is calculated into four directions, a set of GLCM features has been applied such as Energy, Entropy, Contrast, Variance, Homogeneity, Correlation, Sum Average, Sum Entropy, Sum Variance, and Dissimilarity.

GLCM features are classified into two categories: one related to the contrast of texture images and the other related to order of texture images. The first group includes Contrast, Homogeneity, and Dissimilarity, whereas the second group is obtained from Energy, Variance, and Entropy.

In this thesis, GLCM features of off-line signatures I_1 was calculated into four directions and specified as

$$f_l(i,j,d,0^o), f_l(i,j,d,45^o), f_l(i,j,d,90^o), f_l(i,j,d,135^o) \quad (3.50)$$

where f_l infers to GLCM features applied to off-line signature images I_1 in four directions.

In order to calculate the effect of group GLCM on off-line signature texture, contrast and order group are taken into account. And these two groups have been applied separately to off-line signature images.

Figure 3.9 indicates the four direction GLCM feature texture calculation of genuine and forged signature in our database. In this example, the ten GLCM features in 4 directions had been calculated. GLCM features in this example show the performances of each GLCM features on off-line signature images in four directions. Eight features except variance and sum average had the significant difference between genuine and forged signatures. These two GLCM features might not give good performances for off-line signature verification later.

3.5.3 Gabor filters applied for off-line signature verification

Gabor filters or Gabor wavelet is a texture descriptor which can capture salient visual features that may appear at different scales and orientations which was mentioned in previous section.

We applied the Gabor filter for off-line signature images similar to works of Gabor filters (H B Kekre, 2010) (Xue Ling, 2010)]. In our work, off-line signature images after preprocessing are divided into blocks with size $S - by - S$ where S is the size of each block; the frequency β is set by experiment. In this work, we have consulted the research of other work (H B Kekre, 2010) and set $\beta = \frac{1}{8}$. The

values $\sigma_x = 50, \sigma_y = 50$ are empirically set (H B Kekre, 2010). With even S, magnitude calculation of each Gabor filter is shown as

$$g_l(x, y, \theta_k, \sigma_x, \sigma_y) = \left| \sum_{x_o=-\frac{S}{2}}^{\left(\frac{S}{2}\right)-1} \sum_{y_o=-\frac{S}{2}}^{\left(\frac{S}{2}\right)-1} I_{op}(x + x_o, y + y_o)\, hg(x_o, y_o, \theta_k, \beta, \sigma_x, \sigma_y) \right|, \quad (3.51)$$

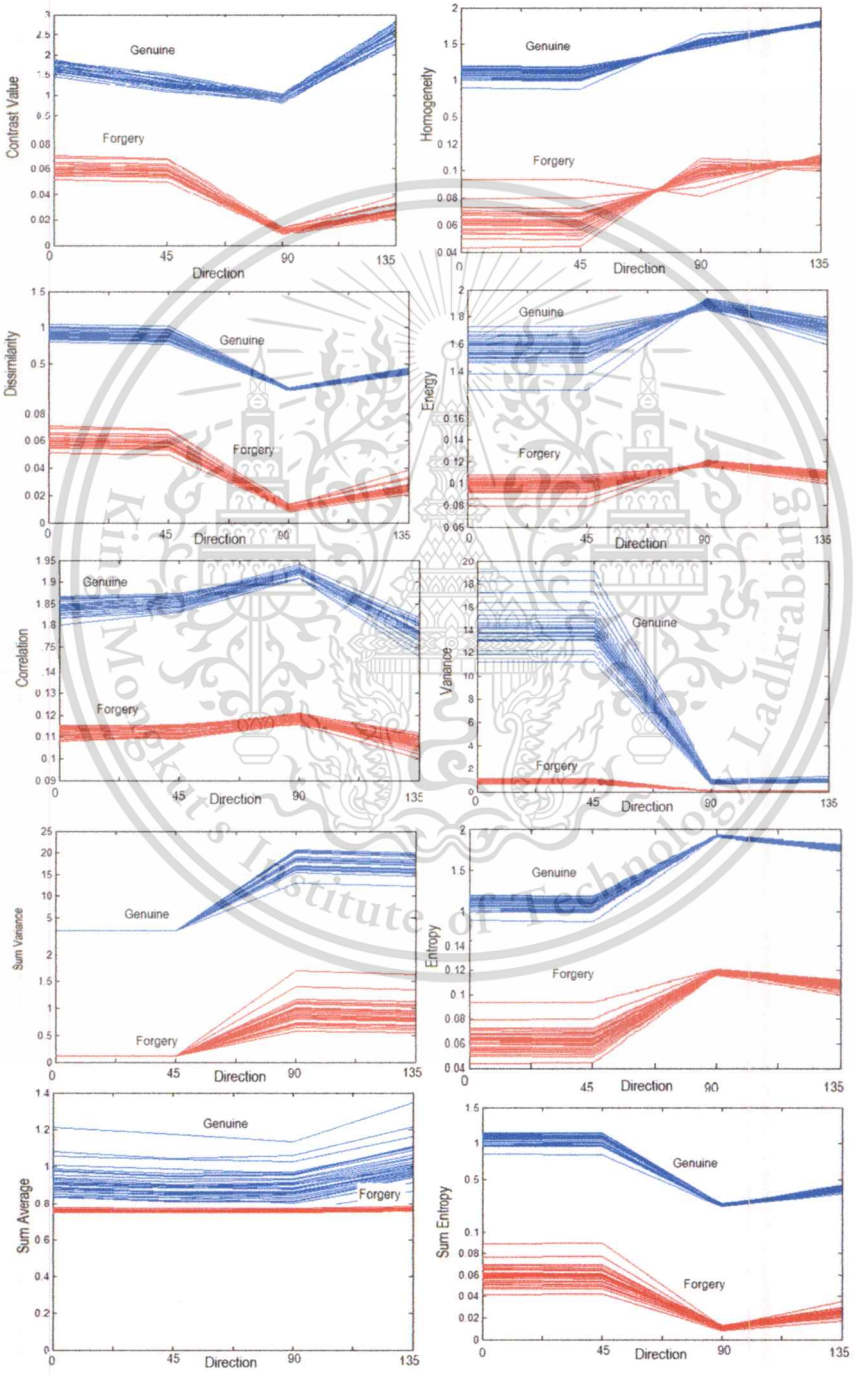

Figure 3.9 GLCM features for genuine and forged signature

In equation 3.51, I(x,y) is grey level of pixel (x,y) of image I_{op}, g_l is the magnitude obtained from each block of the off- line signature image. The feature extraction related to Gabor filters for off-line signature verification is given. In this work, we employ the feature extraction method in (J. F. Vargas M. F., 2010) in which the features are calculated by the mean and range of Gabor filter magnitude. Mean of Gabor magnitude is obtained by

$$Mg_i(l) = \frac{g_{l_i}}{\sum_{i=1}^{N} g_{l_i}}, \tag{3.52}$$

where $Mg_i(l)$ is the mean of Gabor magnitude in the $i-th$ block of the whole off-line signature image, g_{l_i} is magnitude of the corresponding block of the whole off-line signature image. Range of Gabor magnitude is calculated by

$$Rg_i(l) = \frac{g_{l_i} - \min(g_{l_i})}{\max(g_{l_i}) - \min(g_{l_i})}, \tag{3.53}$$

where $Mg_i(l)$ *and* $Rg_i(l)$ are components of feature vector [**Mg**, **Rg**] for each off-line signature image, respectively. Figure 3.10 shows Gabor filter features for genuine and forged signatures in our database. It can be seen that the significant difference between genuine and forged features, thus, these features can be used to verify genuine and forged signatures.

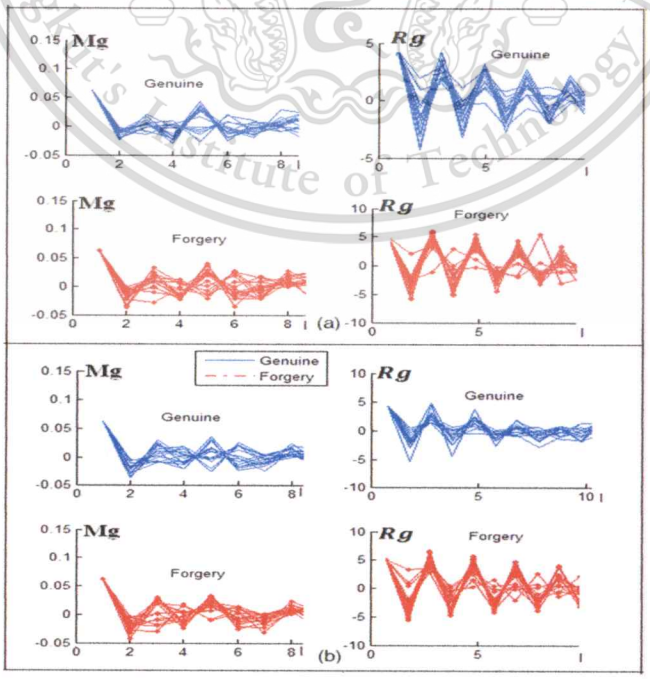

Figure 3.10 Gabor filter features of person (a) and (b) in our database

3.5.4 Local phase quantization for off-line signature verification

The theory and definition of local phase quantization (LPQ) are presented in previous section.

In this work, to apply LPQ for off-line signature texture, we define feature vectors by two outputs of LPQ. They are histogram $\boldsymbol{hi} = hist(\boldsymbol{B}(\boldsymbol{d_r}))$ and sum $\boldsymbol{b} = sum(\boldsymbol{B}(\boldsymbol{d_r}))$. In this thesis, the default span $r = 3$ was applied.

Figure 3.11 shows local phase quantization features for genuine and forged signatures in our database. In this case, the genuine features are blue and red dotted lines are of forgery. It is easy to see that genuine features are much more stable than forgery ones. Therefore, these features can be used as distinguishing features for off-line signature verification and can be representatives for genuine and forged signatures in verification phase.

There are four methods are used for off-line signature verification in this thesis. The first method is gray level change detection for off-line signature verification in which the authentic and forged signatures are verified by finite impulse response (FIR) systems characterizing gray level change of each signature. The second method is GLCM, the features of GLCM are conducted to generate feature vectors served for off-line signature verification. The third was the feature vectors which are extracted Gabor filters, and the fourth method was LPQ feature extraction.

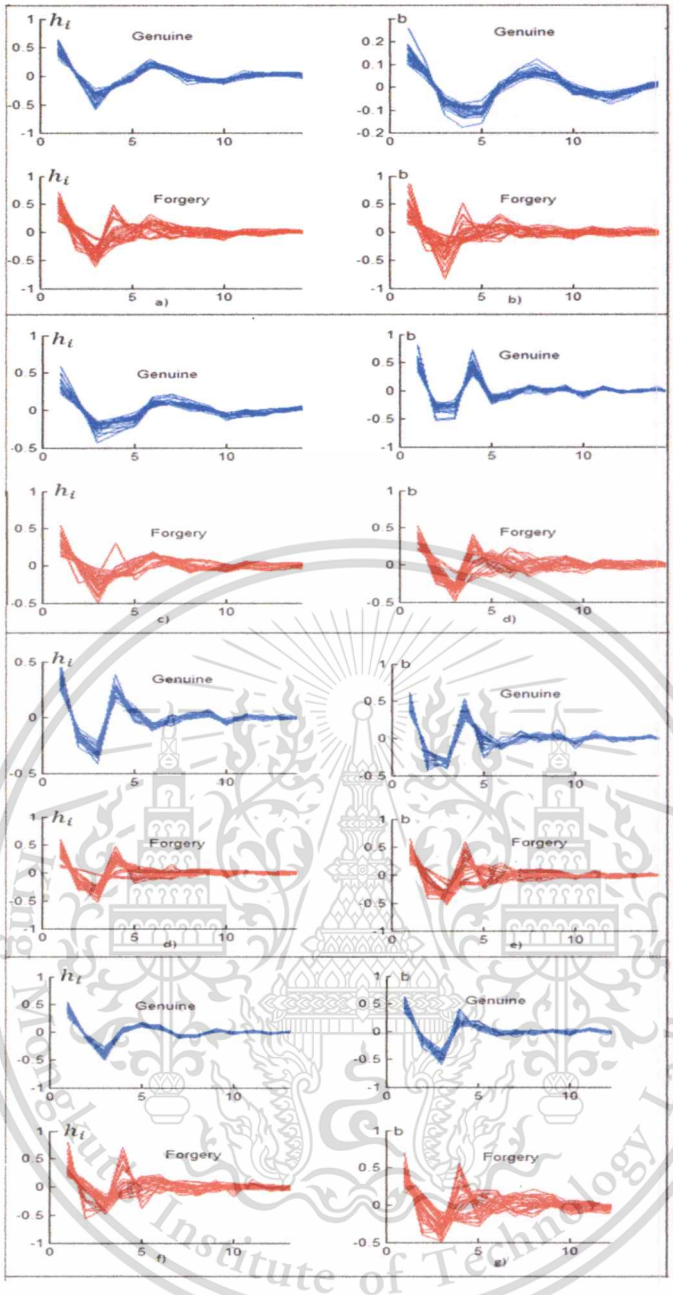

Figure 3.11 Local phase quantization features for four people in our database

Chapter 4

Off-line Signature Verification and Experimental Results

Promising performance results were obtained from our off-line signature verification system. After preprocessing and feature extraction to extract the feature vectors of each signature, signatures are classified into two classes: genuine and forged signatures. Euclidean distance is used for classification in verification off-line signatures. Four methods have been presented thus far; moreover, in this chapter the feature vectors obtained from corresponding feature extractions are shown and the similarity between genuine and forgery signatures is calculated.

4.1 Feature vectors

Feature vectors are calculated differently in that each calculation belongs to the method that is applied to that part. The details on feature vector calculation will be presented in the experimental result section.

4.2 Verification phase

In the verification phase, genuine and forged signatures are verified by the Euclidean distance calculation as described below. Each signature is verified as follows

Genuine if $|| \quad \mathfrak{h}^{(ref)} - \mathfrak{h} \quad || < \xi$; otherwise, forged.

where $\mathfrak{h}^{(ref)}$ is the reference feature vector, $\mathfrak{h}$ is the test feature vector for a particular signature, $||.||$ means "Euclidean norm", and ξ denotes prescribed threshold. There are five reference data in each distance calculation session. The feature vectors which are extracted from the methods in the previous chapter are shown. The verification distance calculation between feature vectors is measured to verify authentic and forged signatures.

4.3 Equal error rate calculation

This section discusses different error rates and explains how to compare the performances of two methods using the same error rate calculation method.

In the evaluation of the performance of a signature verification system, two major factors should be considered: the false reject rate (FRR) of genuine signatures which occurs when an authentic signature is rejected, and the false acceptance rate (FAR) of forged signatures which takes place when forgery signature is accepted. Thus, it is common to talk about the equal error rate (EER) which is the point at which FAR equals FRR as shown in following figure

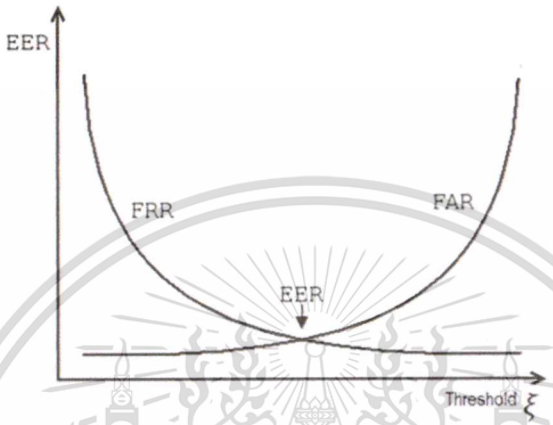

Figure 4.1 Equal Error Rate

In case of the score distributions overlap, the FAR and FRR intersect each other at a certain point. The values of FAR and FRR at that point are called the equal error rate (EER). When comparing two biometric performances, the researchers provide the values of FAR and FRR, the value of EER will be given then. The EER of a system can be used to give an independent performance measurement, the lower EER, the better the system performance. The EER can vary depending on the distributions of the particular method; the final error rates will be different due to the obtained results from FAR and FRR.

Figure 4.2 shows an example of Euclidean distance calculation for verification phase in our database and the corresponding EER. The EERs were calculated case by case and ranged from the highest value of 35% to the lowest of 0%. In this example, the blue circles refer to genuine signatures and red stars are forged ones.

4.4 Experiments

a) The first experiment was performed on FIR characterizing gray level change of off-line signature images. Feature vectors in case of gray level change are the impulse responses obtained from two FIR systems as follows:

- We define the vectors as below:

$$\mathfrak{h}'_1(m) = [h_1(0), h_1(1), h_1(2), \dots h_1(m)], \quad (4.1)$$

$$\mathfrak{h}'_2(m) = [h_2(0), h_2(1), h_2(2), \dots h_2(m)], \quad (4.2)$$

In this case, $[\ h_1(0), h_1(1), h_1(2), \dots h_1(m)]$ and $[h_2(0), h_2(1), h_2(2), \dots h_2(m)]$ are components of vectors obtained from the two FIR systems.

- Feature vectors are obtained from

$$\boldsymbol{k}'(m) = [\mathfrak{h}_1{}'\ \mathfrak{h}_2{}'\ ], \quad (4.3)$$

Each signature will be represented by these feature vectors in verification phrase.

b) The second experiment was GLCM feature extraction, three sub experiments are performed

- In the first sub experiment, according to the work of (Hall-Beyer, 2007), we divided GLCM features into 2 groups, contrast group and order group. Therefore, in this case the feature vectors are defined as

$$\boldsymbol{h}_1 = [contrast, homogeneity, dissimilarity] \quad (4.4)$$

$$\boldsymbol{h}_2 = [energy, entropy, variance] \quad (4.5)$$

- In the second sub experiment, the feature vector is defined by the individual GLCM texture feature vector as

$$\boldsymbol{h}_3 = [contrast, homogeneity, dissimilarity, energy, correlation, \quad (4.6)$$
$$variance, sum\ variance, entropy, sum\ average, sum\ entropy]$$

- In the third sub experiment, from the results of second experiment, we eliminated some ineffective GLCM features to increase the performance of our experiments

$$\boldsymbol{h}_4 = [contrast, homogeneity, dissimilarity, energy, correlation, \quad (4.7)$$
$$entropy, sum\ variance, sum\ entropy],$$

c) The third experiment was on Gabor filters. In this experiment, the feature vector is defined by Gabor filters. They are mean values and range values of Gabor filters magnitude as

$$\boldsymbol{h'_m = [Mg', Rg'],} \tag{4.8}$$

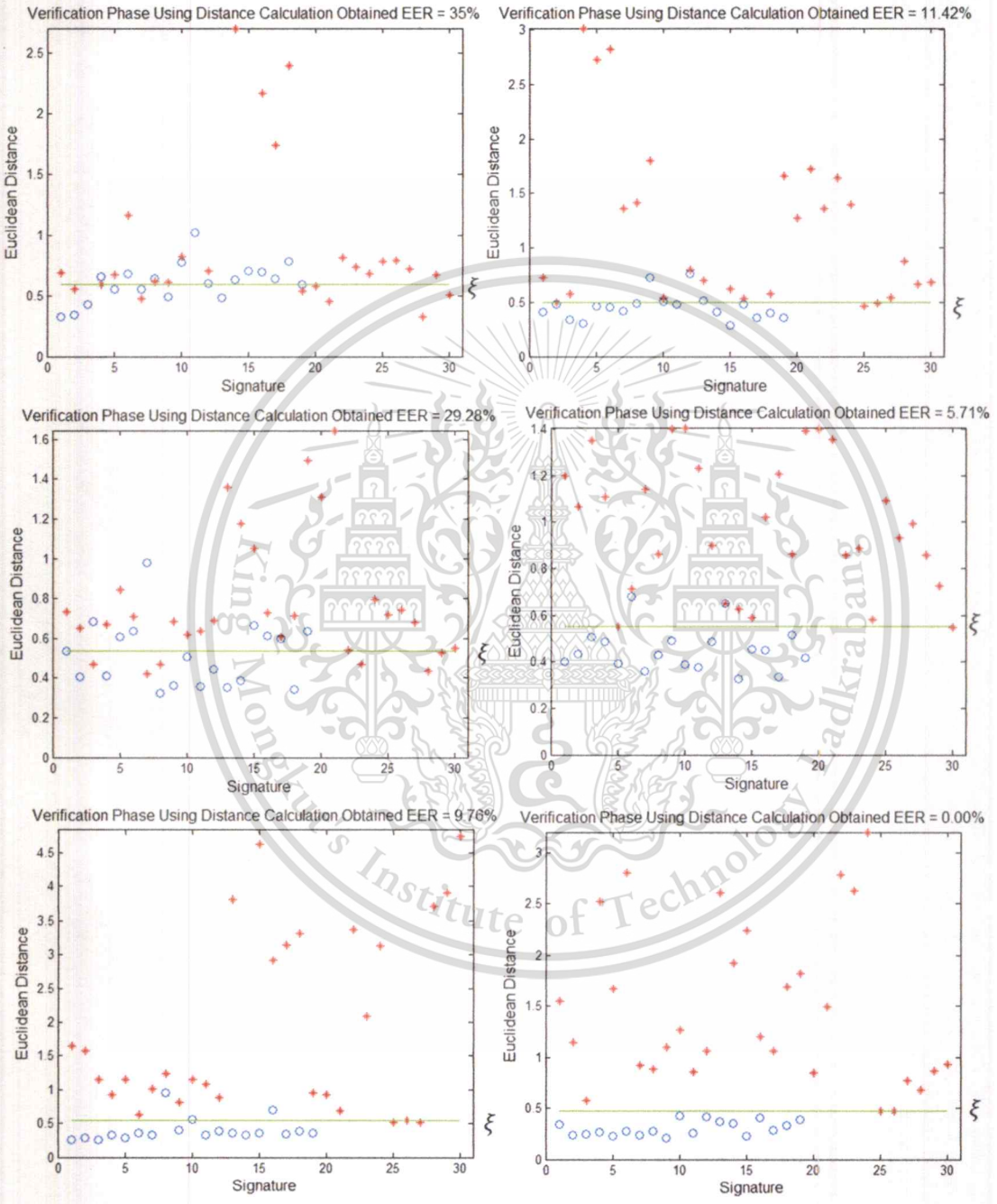

Figure 4.2 Euclidean Distance Examples

where $\boldsymbol{Mg}$ and $\boldsymbol{Rg}$ are two feature vectors obtained from off-line signature images which are mentioned in the over view theory about Gabor filters in previous chapter.

d) The fourth experiment, the feature vector $\boldsymbol{h'_m}$ is defined by local phase quantization (LPQ) as

$$\boldsymbol{h'_m} = [\boldsymbol{hi'}, \boldsymbol{b'}], \tag{4.9}$$

where $\boldsymbol{hi'}, \boldsymbol{b'}$ are average of histogram LPQ and sum feature of LPQ.

4.5 Experimental results

The Equal Error Rate (EER) results given by our proposed methods are shown in table 4.1. From table 4.1, we can see the performances from the first method to the last one have been improved significantly. The FIR system characterizing gray level change method of signature image obtained the EER is 9.35%.

Table 4.1 Results of our proposed methods in %

Method	EER(%)
FIR system characterizing gray level change of the images	9.35
GLCM	6.47
Gabor filters	6.15
Local phase quantization (LPQ)	6.09
Work (F. Vargas, 2010)	13.82

The second method with texture analysis from GLCM and its features had EER was 6.47%. For the third and last method from Gabor filter and LPQ, the EERs were 6.15% and 6.09%, respectively. These results reflect the efficiency of our proposed methods related to texture analysis for off-line signature verification. The EER results when applying GLCM features for off-line signature texture show us that two GLCM features are not effective for off-line signature textures. For more detail, feature variance and sum average given the EER results 14.3277% and 23.9068%, respectively; therefore, these results are not suitable to apply these GLCM features for off-line signature verification. The average of other GLCM features given EER equals 6.47%. Compare with work of (F. Vargas, 2010) on the same database, the EER of their methods were 13.82% which was higher than ours. Therefore, our work in this thesis, we have added more effective methods for off-line signature verification.

4.6 Time consumption calculation

Since many methods have been applying for off-line signature verification, the time calculation consumption is used to calculate usage time of each method. In total, time consumption of the four methods can be depicted in Figure 4.3.

Figure 4.3 shows CPU time consumption comparison of gray level change, GLCM, Gabor filters and LPQ. This figure shows the needed time consumption for a signer. From the figure, we can see that the least time consumption was Gabor filter method in which it takes merely slightly over 9 seconds to verify a signer. With the similar time consumption calculation, the second least time consumption was GLCM, the third one gray level change. On the whole, the most time consumption method was LPQ in which to verify a signer, it took more than 57 seconds.

The results after applying the methods of the previous chapter are presented. The performances of our proposed methods are compared to conclude the better performance among these methods. In addition, the time consumption of each signature is measured to show the more practical method for off-line signature verification in real circumstances.

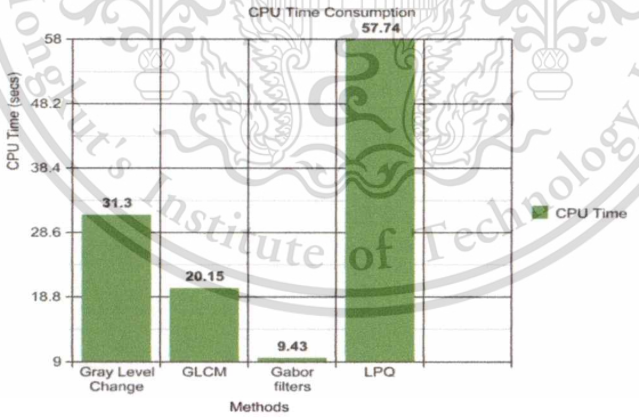

Figure 4.3 Time consumption comparison

Chapter 5

Conclusion

In this thesis we have addressed the problem of handwritten off-line signature verification and improved the quality of signature image by preprocessing and approached their individual features with some effective methods. Four methods, i.e., FIR characterizing grey level change of signature image, GLCM, Gabor filters and LPQ, have been presented for off-line signature verification. These four methods have been employed using the similar preprocessing, and the error rate calculation method by the signature verification experiment on the signature public database which includes 253 signers supplied by (J. F. Vargas M. A., 2007). The verification was conducted for both genuine and forged signatures. The difference among these methods is feature extractions, feature vectors and the error rates by the signature verification experiments are given by corresponding methods.

Gray level occurrence matrix (GLCM), Gabor filters, and local phase quantization (LPQ) are three famous texture analysis methods which have been applied in many studies to discriminate the different regions or to classify texture of images. With off-line signature texture images, these well-known methods have been first studied to verify genuine and forged signatures on a public database.

Genuine and forged signatures in our work have been detected by various methods to determine the most effective method for off-line signature verification. Off-line signatures are easier to forge; hence, the performance of off-line signature verification system is always lower than that of on-line signature system. However, the results obtained from texture analysis methods have improved performances of off-line signature verification and it shows that texture analysis is an effective way to off-line signature verification.

Despite lack of dynamic characteristics such as pen-tip coordinates, velocity, pen up, pen down, the our proposed texture analysis methods that have applied to off-line signature images provided better error rates compared to other works on the same database as shown in Table 4.1. Specifically, the final error rate obtained from the local phase quantization was 6.09%. This shows that the performance of off-line signature can be as good as on-line signature system.

Comparison among our own methods, the experiment results show that our obtained EERs have been improved from 9.35% to 6.09%.

The future works for off-line signature verification is more investigated about incomplete signature image or the signature image includes with much noise.

Publication List

***"Off-line Signature Verification based on FIR System Characterizing Gray Level Change"*- Nguyen thi Minh Nguyet**, Pittak Thumwarin, Takenobu Matsuura - JSTT 2011 International Conference on Modelling and Simulation Techonology (JSST2011), pp. 460-463.

***"Off-line signature verification using Gray level Co-occurrence Matrix Texture Analysis"* - Nguyen thi Minh Nguyet**, Pittak Thumwarin, Takenobu Matsuura - 1st International Symposium on Technology for Sustainability (ISTS2011).

"Off-line Signature Verification Using Local Phase Quantization and Gabor filter texture feature" - **Nguyen thi Minh Nguyet**, Pittak Thumwarin, Takenobu Matsuura – ASEAN Engineering Journal (submitted).

Bibliography

A. K. Jane, A. R. (2004). An introduction to biometric recognition. *IEEE transactions on circuits and systems for video technology, Vol. 14, No. 1.*

Abbas, R. (1994). *A prototype system for off-line signature verification using multilayered feedforward neural networks.*

Authority, N. F. (n.d.). *http://www.cumbria.police.uk*. Retrieved from Bank Card and Cheque Fraud: http://www.cumbria.police.uk/admin/uploads/attachment/files/Advice_and_Info/Fraud/Bank_Card_and_Cheque_fraud.pdf

B. Kovari, Z. K. (2007). Off-line signature verification based on feature matching. *IEEE.*

B.H. Shekar, R. B. (2011). eigen-signature: A robust and an efficient offline signature verification algorithm . *ICRTIT.* Chennai: IEEE.

Berisha, S. (2009, May). Image classification using Gabor filters and Machine Learning. Winston-Salem, North Corolina.

Berisha, S. (2009, May). Image Classification Using Gabor Filters and Machine Learning . *Master Thesis*. Winston-Salem, Corolina.

D. Kumar, Y. R. (2009). A brief introduction of biometrics and fingerprint payment technology. *International of Advance Science and Technology*, 25-38.

E. Ozgunduz, T. S. (n.d.). Off-line signature verification and recognition by support vector machine .

fraud, I. a. (2012). *Stopcheckfraud*. Retrieved from stopcheckfraud.com: http://www.stopcheckfraud.com/statistics.html

Gabor, D. (1946). Theory of Communication . *Bristish Thomson-Houson Co., Ltd., Research Laboratory*, 429-457.

H B Kekre, V. A. (2010). Gabor filter based feature vector for Dynamic Signature Recognition. *International journal of Computer Applications*, 74-80.

H B Kre, V. A. (2009). Fingerprint and Palmprint Segmentation by Automatic Thresholding of Gabor Magnitude. *ICETET-09*, 235-241.

Hall-Beyer, M. (2007, February). *The GLCM Tutorial Home Page*. Retrieved from http://www.fp.ucalgary.ca/mhallbey/tutorial.htm

J. F. Vargas, M. A. (2007). Off-line Handwritten Signature GPDS-960 Corpus. *IAPR 9th International Conference on Document Analysis and Recognition* (pp. 764-768). ISBN: 978-0-7695-2822.9.

J. F. Vargas, M. F. (2010). Off-line signature verification based on grey level information using texture features. *ScientDirect* (pp. 375-385). Elsevier.

J. Ruiz-del-Solar, C. D. (2008). Off-line signature verification using local interest points and descriptors. Berlin: Springer-Verlag Berlin Heidelberg .

J. Ruiz-del-Solar, C. D. (2008). Off-line signature verification using local interest points and descriptors . *CIARP* (pp. 22-29). Springer-Verlag.

J. Y. Tou, Y. T. (n.d.). Gabor filters and Grey level Co-Occurrence Matrix in Texture Classification.

J.F Vargas, M. F. (2007). Off-line Handwritten Signature GPDS-960 Corpus. *International Conference on Document Analysis and Recognition*, (pp. 764-768). Brazil.

Katrin Franke, S. R. (2004). Ink Deposition Model: The relation of writing and ink deposition processes. *Proceedings of the 9th Int'l workshop on Frontiers in Handwriting Recognition* .

Kholmatov, A. A. (2003). Biometric Identity Verification Using On-line & Off-line Signature Verification. *Master Thesis*. Alisher Analolyevich Kholmatov 2003.

L. Soh, C. T. (1999). Texture analysis of SAR Sea Ice Imagery Using Gray Level Co-occurrence Matrix. *IEEE Transactions on Geoscience and Remote Sensing* , (pp. 780-794).

M. A. Ferrer, F. V. (2010). Signature verification using local directional pattern(LDP).

M. A. Ferrer, J. F. (2012). Robustness of Off-line signature Verification based on Gray Level Features. *IEEE Transactions on Information forensics and Security* , 966-977.

M. M. Mokji, S. A. (2007). Gray level Co-occurrence matrix Computation Based on Haar Wavelet. *CGIV 2007.* Computer graphics, Imaging and Visualisation.

M.B Yilmaz, B. Y. (2011). Offline signature verification using classifier combination of HOG and LBP features. IEEE.

Morse, B. (1998-2000). *Texture.* Brigham Young University.

Nguyen thi Minh Nguyet, P. T. (2011). Off-line signature verification using Gray level Co-occurrence matrix Texture Analysis . *ISTS.* Bangkok: KMITL.

Panton, M. S. (2010, December). Off-line signature verification using essembles of local Radon transform-based HMMs. University of Stellenbosch.

Pitak Thuwarin, N. t. (2011). Offline signature verification based on FIR system characterizing gray level change. *JSST* (pp. 5-10). Japan: JSST2011.

R. Larkins, M. M. (2008). Adaptive feature thresholding for off-line signature verification .

R.M Haralick, K. S. (1973). Textural features for image classification. *IEEE transactions on systems, Man and Cybernetics*, 610-621.

S. Brahnam, L. N. (2010). Local phase quantization texture descriptor for protein classification. *BioComp'10*, (pp. 159-165).

S. Brahnam, L. N.-Y. (2010). Local phase quantization texture descriptor for protein classification. *Bioinformatics and Computational Bilogy*, 159-165.

S. Lee, J. P. (1992). Offline tracking and representation of signatures. *IEEE transactions on System.* Man and Cybernetics 22.

Simon Liu, M. S. (2001). A practical guide to biometric security technology. *IEEE*, (pp. 27-32).

V. Ojansivu, E. R. (2008). Rotation Invariant Local Phase Quantization for Blur Insensitive Texture analysis.

V. Ojansivu, J. H. (2008). Blur Insensitive Texture Classification Using Local Phase Quantization. *ICISP2008* (pp. 236-243). Springer-Verlag Berlin Heidelberg.

Westpac. (2006). *http://www.westpac.com.au*. Retrieved from Prevent check fraud: http://www.westpac.com.au/docs/pdf/aw/Prevent_cheque_fraud.pdf

Xue Ling, Y. W. (2010). On-line Signature Verification Based on Gabor Features. *IEEE*.

Y. Qiao, J. L. (2007). Offline signature verification using online handwriting registration. *IEEE*.

Z. Wang, B. A. (2002). Why is image quality assessment so difficult? *Acoustic, Speech and Signal Processing* (p. volume 4). IEEE International Conference.

JSST

30th JSST Annual Conference (JSST 2011)

International Conference on Modeling and Simulation Technology

PROCEEDINGS

October 22-23, 2011

Tokai University Takanawa Campus, Tokyo, Japan

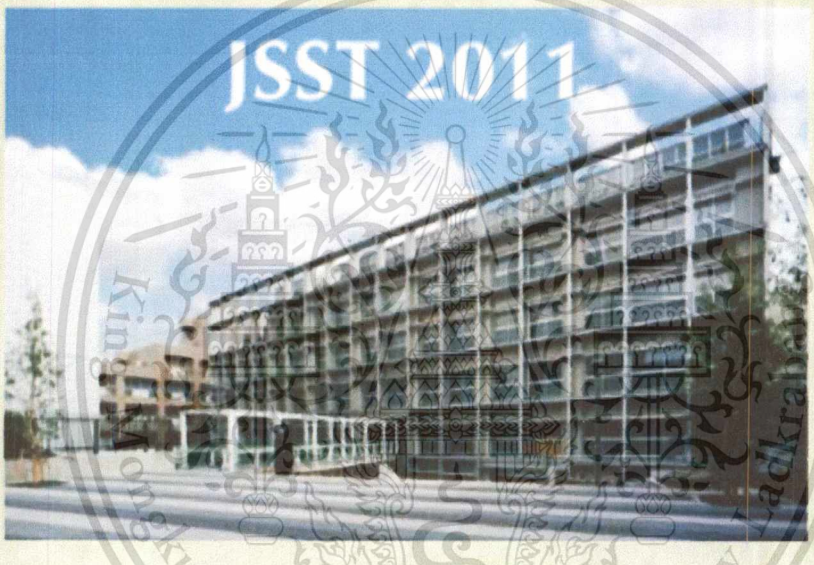

Japan Society for Simulation Technology (JSST)

International Conference on Modeling and Simulation Technology
October 22-23, 2011, Tokai University Takanawa Campus,
Tokyo, JAPAN

Off-line Signature Verification based on FIR System Characterizing Gray Level Change

Pittak Thumwarin[1], Nguyen thi Minh Nguyet[1] and Takenobu Matsuura[2]
[1] Faculty of Engineering, King Mongkut's Institute of Technology Ladkrabang, Bangkok, 10520 Thailand.
E-mail: ktpitak@kmitl.ac.th
[2] School of Engineering, Tokai University, 1117 Kitakaname, Hiratsuka, Kanagawa, 259-1292, Japan.
E-mail: matsuura@tokai.ac.jp

Abstract— In this study, we propose off-line signature verification based on finite impulse response (FIR) system characterizing gray level change of the off-line signature image. Two FIR systems are used to represent the handwriting system. In the first FIR system, the discrete cosine transforms (DCTs) of the gray level change and histogram of the signature images are used as input and output of the FIR system, respectively. For the second FIR system, the DCTs of gray level change at the border of signature and its slope are used as the input and output for this system, respectively. The obtained impulse responses of two FIR systems are used as the individual features of the particular signature. Off-line signatures can be verified by evaluating the difference between the impulse responses of two FIR systems obtained from reference and test signatures. The off-line signature verification experiments were performed on the GPDS300GRAY[3] signature database which consists of 6072 genuine signatures and 7495 imitations signed by 253 signers. The error rate of our experiment in proposed method was 9.35%.
Keywords— offline signature, gray level changes, FIR system, discrete cosine transform

1 Introduction

Security is one of the most concern issues in daily life and it plays major role in many applications, the requirement of verification the authentic people are becoming more and more necessary. Many methods are presented to solve this problem in the real life, for instance, iris recognition, finger print verification, gesture recognition, and signature verification. These biometrics are used to identify who are the authentic users and based on their own characteristics to classify the permission to access a particular security system.

Signature verification is conceded as one of the effective techniques to indentify the authentic problems. In practice, signature verification is divided into two main fields; they are on-line signature verification and off-line signature verification. With on-line signature verification, we need special tools to collect signatures of signers, but off-line signatures, users can sign on any surface, and then the images of signatures are used for signature verification.

There are several works on off-line signature verification. In work[1] introduces Adaptive Feature Thresholding (AFT) which is a novel method of person-dependent off-line signature verification. The method in work[2] explores the usefulness of texture based measures with binarized signatures. And work[7] based on global image analysis and a statistical distance measure while the second one is based on local image analysis. Or in work[8], off-line signature verification system based on fusion of two machine experts is presented.

Despite many methods for off-line signature verification have been proposed, it seems that the performances of their methods are not enough for practical usage. In this study, we represent off-line signature verification method based on finite impulse response (FIR) system characterizing gray level change of signature images. In our method, discrete cosine transforms (DCTs) of the features of handwriting are used to reduce fluctuation of the features. Moreover, the FIR system is introduced to represent features and to characterize the handwriting system as well. The obtained impulse response of the FIR system is used as the individual features to verify genuine or forgery signatures.

2 Preprocessing

In this paper, off-line signature images are collected by using scanner. The original images include three components which are main part of signatures, noise and image background. To concentrate on pepper and salt noise elimination, gray level of each image is changed to detect pepper and salt noise. Then a threshold of gray level is applied to separate the main part of each signature and the noise part.

From original images, we detect the gray level and define the threshold by the equation below

$$I_g = round\left(\frac{1}{round\left(\left(\sum_{i=1}^{N}\sum_{j=1}^{M}\frac{I_o * s}{G}\right) * \frac{G}{s}\right)}\right), \quad 1)$$

where I_g refers to grey level change images, I_o indicates original images, s is threshold and G is gray level of original image. $round$ function in equation 1 to guarantee the obtained result is integer.

Based on this gray level change images, we create binary mask with the condition follow:

$$If\ I_g = 255\ then\ I_{bw} = 255\ else\ I_{bw} = 0,$$

In the above equation, I_{bw} is binary image.

And the binary mask is used to cover the main part of original images by below condition:

$$If\ I_{bw} = 255\ then\ I_{op} = 255\ else\ I_{op} = I_o,$$

I_{op} is the off-line signatures which we derive from preprocessing. An example of our preprocessing process is shown in Fig. 1.

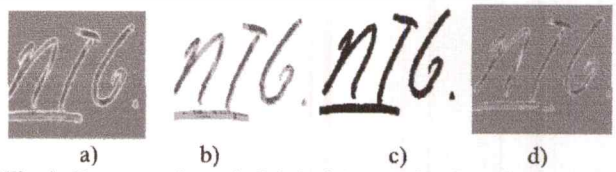

a) b) c) d)

Fig 1. Preprocessing; a) Original image; b) Gray level change image; c) Binary image; d) Image after preprocessing

3 Feature Extraction

3.1 Gray level and border of signature features

For off-line signature verification, shape of signature is one of the most important features to verify random forgery signatures who sign without any information about authentic signatures. However, for skill forgers who have seen genuine signatures and their forgery signatures are almost similar with genuine ones.

Therefore, only considering shape of signature to verify between genuine and forgery signatures is not always effective.

In this paper, in order to verify the skill forgery signatures, the features related to gray level change of signature images are taken into account. In this case, four features are extracted and divided into two groups. For the first group, the features are extracted from the whole signatures. For the second group we concentrate on the gray level change along the border of each signature.

In the first group, gray level change and histogram features of signature images are detected. To extract gray level features of each signature, each signature is divided into fixed size blocks. The difference between the summations of gray levels of two adjacent blocks of signature image as shown in Fig. 2 is calculated as follows:

$$g(k) = \sum_{i=1}^{M}\sum_{j=1}^{N} B_k(i,j), \qquad 2)$$

$$f_i = g(k+1) - g(k), \qquad 3)$$

where $[M, N]$ is sizes of blocks, k is the index of block and $B_k(i,j)$ is gray level of block k^{th} at the position i, j, respectively. The first feature can be determined by connecting together the feature f_i as vector $\boldsymbol{f}' = [f_1, f_2, f_3, \dots f_n]$, n is the number of blocks.

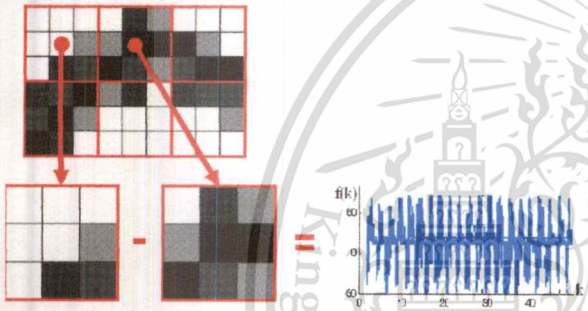

Fig 2. Gray level change of off-line signature based on two adjacent blocks

The second feature of gray level of each signature, histogram $\boldsymbol{t}' = [t_1, t_2, \dots, t_n]$ of off-line signature image is calculated. Fig. 3 is one example of histogram feature extraction.

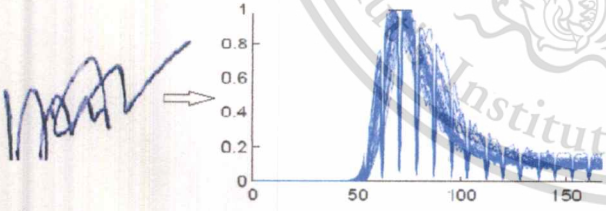

Fig 3. Histogram of off-line signature image

In the second group, the gray level change along each signature's borders and its slopes are determined.

For the third feature in group two, the features of handwriting related to gray level change at the border of signatures are extracted. In this case, the borders at the top, left, bottom and right of signature are detected. The third feature of handwriting is defined as $\boldsymbol{b}' = [b_1, b_2, \dots, b_n]$ by the combination of gray level at the border of signatures. The example of the third feature is shown in Fig. 4.

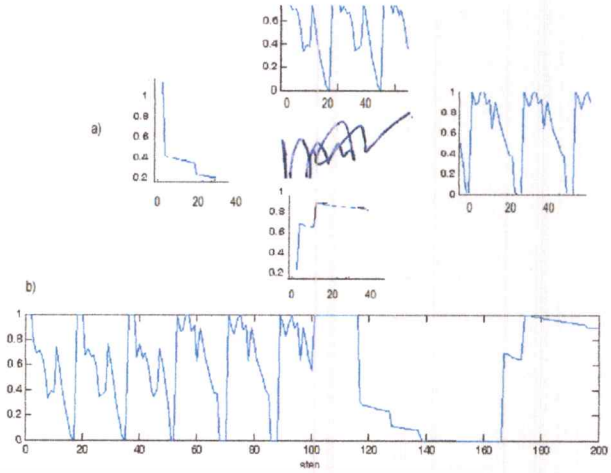

Fig 4. Border extraction of off-line signature image; a) off-line signature image with feature extracted from four sides; b) the gray level of four sides are presented in one graph.

Finally, it is observed that off-line image signatures signed by different pens are different. In order to extract consistent feature of handwriting, the fourth feature of handwriting is determined by calculating slopes of gray level at borders of signatures $\boldsymbol{s}' = [s_1, s_2, \dots, s_n]$.

Fig. 5 shows examples of four features of handwriting obtained from genuine signatures and forgeries for person A and person B in our database.

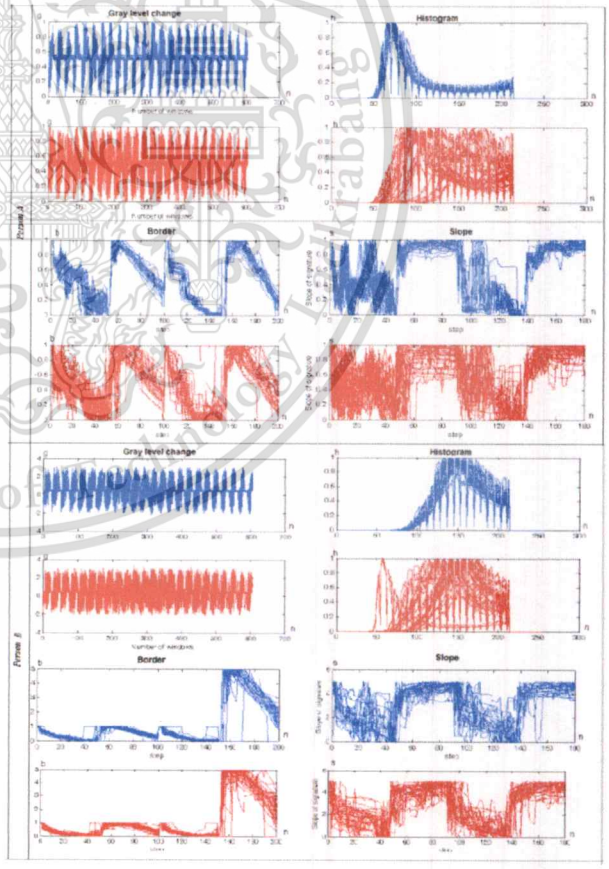

Fig 5. Features $\boldsymbol{f}$, $\boldsymbol{t}$, $\boldsymbol{b}$, $\boldsymbol{s}$ obtained from person A and person B

3.2 Discrete Cosine Transform of the feature of the signature

In order to reduce the fluctuations of features of handwriting, discrete cosine transforms (DCTs) for each feature vector are calculated by using the equation 4 as follows:

$$\Psi_{\varpi} = \sqrt{\frac{2}{M}}\mu(m)\sum_{n=0}^{M-1}(q(t)cos[\frac{\pi(2n+1)m\pi}{2M}]), \quad 4)$$

$$\mu(m) = 1(m \neq 0), \mu(0) = \frac{1}{\sqrt{2}},$$

$$m = 0, 1, 2, \ldots M-1, \varpi = \boldsymbol{f}, \boldsymbol{t}, \boldsymbol{b}, \boldsymbol{s}$$

Fig. 6 illustrates examples of DCTs of the four features obtained from four features. It can be seen from features that the fluctuations can be reduced by using DCTs.

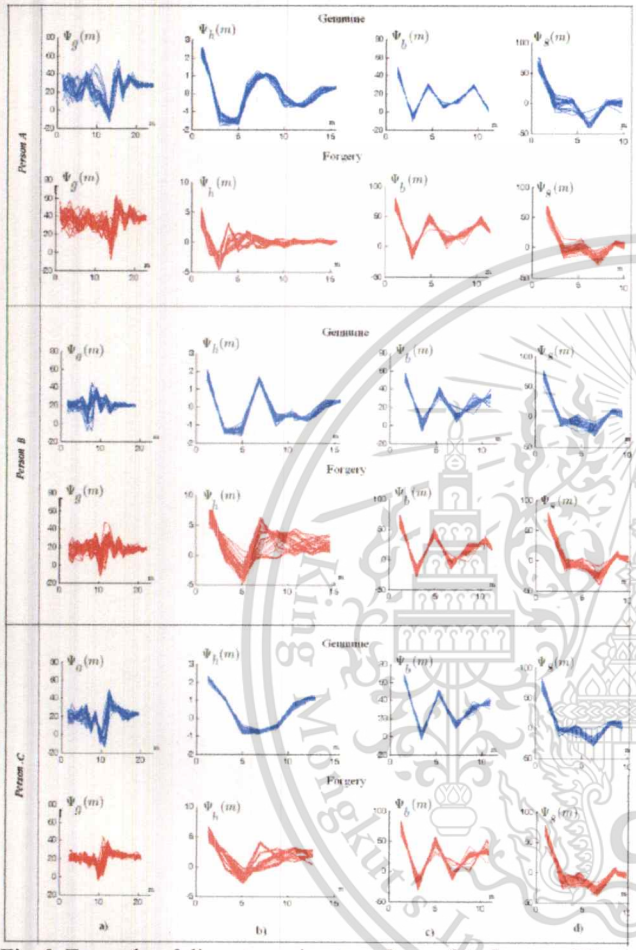

Fig 6. Example of discrete cosine transform of 3 signers; a)First feature; b) Second feature; c) Third feature; d) Fourth feature

3.3 Finite impulse response system characterizing gray level change of signature

In order to characterize the gray level change of the signature, two FIR systems are introduced to describe features of handwriting. In the first FIR system, $\Psi_h(m)$ and $\hat{\Psi}_g$ are used as input and output of the system, respectively. In the second FIR system, $\Psi_s(m)$ and $\hat{\Psi}_b$ are used as input and output system. Two FIR system mentioned above are represented follows:

$$\hat{\Psi}_g(k) = \sum_{m=0}^{M} \mathfrak{h}_1(m)\Psi_h(k-m), \quad 5)$$

$$\hat{\Psi}_h(k) = \sum_{m=0}^{M} \mathfrak{h}_2(m)\Psi_s(k-m), \quad 6)$$

where $\mathfrak{h}_1(m)$ and $\mathfrak{h}_2(m)$ are the impulse response of two FIR systems, respectively. M is order of the FIR systems. The impulse responses $\mathfrak{h}_1(m)$, $\mathfrak{h}_2(m)$ can be determined by minimizing the least-square error at M as:

$$\mathcal{E}_1 = \sum_{m=0}^{M}[\Psi_g(m) - \hat{\Psi}_g(m)],^2 \quad 7)$$

$$\mathcal{E}_2 = \sum_{m=0}^{M}[\Psi_h(m) - \hat{\Psi}_h(m)],^2 \quad 8)$$

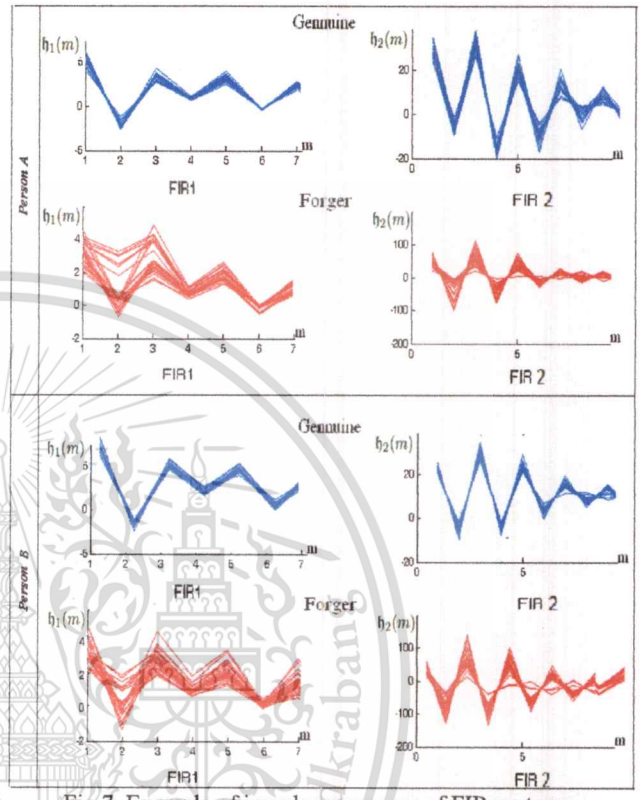

Fig 7. Example of impulse responses of FIR systems

Figure 7 shows the impulse responses $\mathfrak{h}_1(m)$, $\mathfrak{h}_2(m)$ which are obtained from genuine and forgery signatures. It can be seen that the derived impulse responses from genuine signatures are significantly different from the forgery signatures. Therefore, it can be considered that the impulse responses of the two FIR systems can be used as the individual features for off-line signature verification.

4 Experimental results

The impulse responses obtained from the preceding section are used to verify the signatures as follows:

- We define the features vectors as belows:
  $\mathfrak{h}'_1(m) = [h_1(0), h_1(1), h_1(2), \ldots h_1(m)]$, 9)
  $\mathfrak{h}'_2(m) = [h_2(0), h_2(1), h_2(2), \ldots h_2(m)]$, 10)
- Feature vectors are obtained from
  $\mathfrak{h}' = [\mathfrak{h}'_1\ \mathfrak{h}'_2]$ 11)
- Each signature is verified as follow

Genuine if $||\ \ \mathfrak{h}^{(ref)} - \mathfrak{h}\ \ || < \xi$; otherwise, forgery.

where $||.||$ means "Euclidean norm" and ξ means prescribed threshold determined by using training data.

In our experiment, we use public database GPDS300GRAY[3]. which contains 6072 genuine signatures and 7495 imitations signed by 253 signers. And five signatures are selected randomly used as training data. Fig. 8 shows example of Euclidean distance from genuine and forgery signatures.

Comparison of our experimental result with proposed method and some related works[1][2] which used the same database is shown in table 1. In can be seen that, the results in our experiment is better than other works[1][2]. The experimental result shows that our proposed method is effective for off-line signature verification.

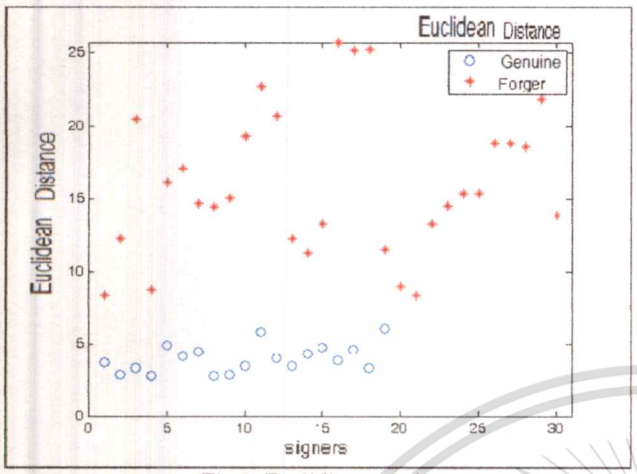

Fig 8. Euclidiean result

Table 1. Comparision of proposed method with work[1] and work[2] in %

Method	*FAR*	*FRR*	*EER*
Proposed	10.0	9.50	9.35
Work[1]	19.50	22.45	21.50
Work[2]	-	-	13.82

5 Conclusion

We propose an off-line signature verification method based on FIR system charactering gray level change of signature images. In the proposed method, four features of handwriting related to gray level of signature images are extracted. The DCTs of four features are used to reduce the fluctuation and extract the individual features of handwriting. Then, the two FIR systems are used to characterize the gray level change of signature images. Finally, the obtained impulses of the two FIR systems are used as unique features for classify genuine and forgery signatures. The experimental result shows that our proposed method is effective for off-line signature verifications.

References

[1] R. Larkins, M. Mayo. *"Adaptive Feature Thresholding for Off-line Signature Verification"*. Proceeding of the IEEE(2008),

[2] Miguel A. Ferrer, Francisco Vargas, Carlos M. Travieso, Jesus B. Alonso, *Signature Verification using Local Directional Pattern (LDP)*, Proceeding of the IEEE(2010),

[3] J. F. Vargas, M. A. Ferrer, C. M. Travieso and J.B. Alonso, *Off-line signature verification based on grey level information using texture features*. Proceeding of the IEEE 67(2010)375-385.

[4] T. Matsuura, M. Takahashi and S. Yamamoto, *"FIR System presentation of chin's shape and its application to personal identification"*

[5] S. Ali Khayam, *"The Discrete Cosin Transform(DCT): Theory and Application"*

[6] Jame. S. Walker, Fourier Series. *"Encyclopedia of Physical Science and Technology"*, Proceeding of the IEEE(2010)

[7]J. Fierrez-Aguilar, N. Alonso-Hermira, G. Moreno-Marquez, and J. OrtegaGarcia. *"An off-line signature verification system based on fusion of local and global information"*. In Workshop on Biometric Authentication, Springer LNCS-3087, pages 298-306, May 2004.

[8] Javier Ruiz-del-Solar, Christ Devia, Patricio Loncomilla, and Felipe Concha. *"Offline Signature Verification Using Local Interest Points and Descriptors"*, CIARP 2008, LNCS 5197, pp. 22–29, 2008. Springer-Verlag Berlin Heidelberg 2008

1st International Symposium on Technology for Sustainability (ISTS2011)

26-29 January 2012, KMITL, Bangkok Thailand

Co-organized by:
Institute of National Colleges of Technology, Japan
and
King Mongkut's Institute of Technology Ladkrabang, Thailand

Off-line Signature Verification Using Gray Level Co-orcurence Matrix Texture Analysis

Nguyen thi Minh Nguyet[‡], Pittak Thumwarin[*], Takenobu Matsuura[†]
Faculty of Engineering[*], International College[‡], King Mongkut's Institute of Technology Ladkrabang [*‡]
Bangkok, 10520 Thailand. E-mail: ktpitak@kmitl.ac.th[*], nguyetnm.it@gmail.com[‡]

School of Engineering[†], Tokai University[†], 1117 Kitakaname, Hiratsuka, Kanagawa, 259-1292, Japan.
E-mail: matsuura@tokai.ac.jp

***Abstract*—Off-line signatures are verified by texture features based on grey level co-occurrence matrix(GLCM). The most well-known texture features which are contrast, homogenety, energy, correlation, variance, inverse diference moment, entropy, sum average and sum entropy are calculated. The significance of these texture features on off-line signature image is detected by four directions $0^0, 45^0, 90^0, 135^0$ of GLCM. The effectiveness of the signature verification using the individual texture feature and their combination are reported. In our study, public database GPDS300GRAY [12] which includes 253 signers, each signer contains 24 genuine and 30 forgery signatures is used for experiments. The final error rates are compared to conclude the most effective GLCM texture feature on off-line signature image, the average error rate is 6.47%.**

***Index Terms*—off-line signature, texture, gray level co-occurrence matrix**

I. Introduction

Security is one of the most concern issues in daily life and plays major role in many applications, the requirement of verification the authentic people are becoming more and more necessary. Many methods are presented to solve this problem in the real life like iris recognition, finger print verification, gesture recognition, and signature verification. These biometrics are used to identify who are the authentic users and based on their own characteristics to classify the permission to access a particular security system.

Signature verification is conceded an effective techniques to indentify the authentic problems. In practice, signature verification is divided into two main fields; they are on-line signature verification and off-line signature verification. For on-line signature verification, we need special tools to collect signatures of signers, but off-line signatures, users can sign on any surface, and then the images of signatures are used for signature verification.

The grey-tone spatial-dependence matrix, or gray level coorcurence matrix(GLCM), which is the statistical relationship of a pixel intensity to the intensity of its neighbouring pixels, has been used for image texture GLCM analysis has been used many texture analysis [2]. The application of GLCM into the texture needs the concern of direction which GLCM is calculated and the size of GLCM as well. Image texture analysis is a more robust method than direct grey-level intensity measurement, because texture is independent of the tones of the images, and image texture contains statistical information in the spatial domain. Some texture descriptors such as angular second moment(energy), entropy, sum entropy and difference entropy invariant to translation, rotation or scaling [5].

There were several works which analyze texture for off-line signature verification such as method based on the microscopic inspection of the writing trace and assumptions about the underlying writing process [11], or work [4] use grey level coorcurence matrix for off-line signature image. In practice for off-line signature verification, work [4] researched on GLCM for off-line signature image by four GLCM texture features, but it seems that using four texture features is not enough for off-line signature verification. In this study, we not only study about the group influence on off-line signature texture, but also the individual texture features with four directions $0^0, 45^0, 90^0, 135^0$ are taken into account. Additionally, the comparison of the effect of individual texture feature and the group texture features are shown. Furthermore, we concern about off-line signature image texture which includes the ink pot and the characteristic of people such as ink contribution, pressure, style of signature or the speed of signer as well. Texture of off-line signature image is analyzed by calculation of the texture features in two case, the first one is based on GLCM with the four directions in the invidiual texture feature case, and the second one is the combination of texture feature. Finally, the suitable texture features are selected and used as feature vector for signature verification.

II. Preprocessing

In this paper, off-line signature images are collected by using scanner. The original images include three components which are main part of signatures, noise and image background. Concentrating on eliminating pepper and salt noise, gray level of each image is changed to detect pepper and salt noise. Then a threshold of gray level is applied to separate the main part of each signature and the noise part. From original images, we detect the gray level and define the threshold by the equation below

$$I_g = round(round(\sum_{i=1}^{N}\sum_{j=1}^{M}\frac{I_0 * s}{G}) * \frac{G}{s}), \qquad (1)$$

where I_g refers to grey level change image, I_0 indicates original images, s is threshold and G is gray level of original

image, *round* function in equation 1 to guarantee the obtained result is an integer. In this study, the gray level of off-line signature image G is 255, and the threshold s is 3.
Based on this gray level change images, we create binary mask with the condition follow:

$$\text{if } I_g = 255 \text{ then } I_{bw} = 255 \text{ else } I_{bw} = 0, \quad (2)$$

In the above equation, I_{bw} is binary image. And the binary mask is used to cover the main part of original images by below condition:

$$\text{if } I_{bw} = 255 \text{ then } I_p = 255 \text{ else } I_p = I_o, \quad (3)$$

I_p is the off-line signatures which we derive from preprocessing. An example of our preprocessing process is shown in Fig.1.

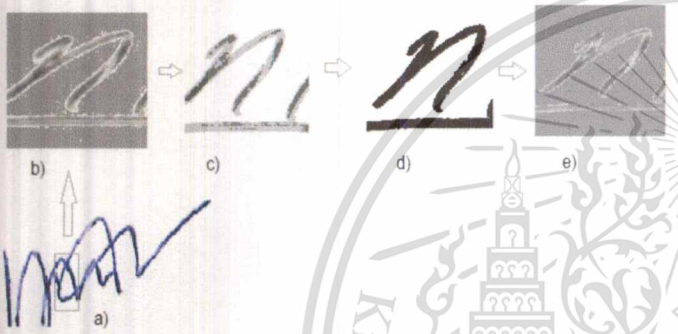

Fig. 1. Preprocessing; a) The whole example signature b) A part of original image; c) Gray level change image; d) Binary image; e) Image after preprocessing

III. Feature Extraction

Applying GLCM and its features for off-line signature image, the grey level of image is changed as the rule mentioned in [4]. In our study, to apply GLCM calculation, the gray level of off-line signature images is changed grey level using the following equation.

$$I = round(\frac{I_p * k}{G}) \quad (4)$$

where I_p is the image obtained from preprocessing step, I is the denotation of image after change the grey, G is grey level of original image signature before GLCM calculation, k is the chosen level to reduce gray level, in our experiment $k = 7$ is acceptable for image with gray level 8. Gray level coorcurence matrix is a method used to extract the texture features of image in a spatial area was publiced in Halick paper [5](1973). Each image texture is calculated by using a set of gray level coorcurence matrix (GLCM) for texture analysis, the GLCM calculates the probilities that a certain grey level of pixel difference in a prescribed direction and a distance from its neighbouring pixels. GLCM is formed in a formula 5 which was presented in [3].

$$P_d(i,j) = |(r,s),(t,v) : I(r,s) = i, I(t,v) = j|, \quad (5)$$

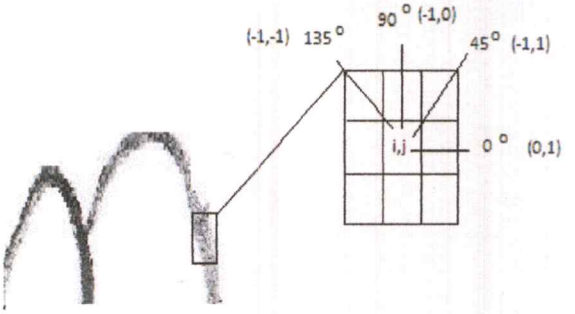

Fig. 2. Neighboring pixels with 4 directions

where $(r,s),(t,v) \subset NxN$, (i,j) is the interest pixel, $P_d(i,j)$ is GLCM due to the direction d, $(t,v) = (r + dx, s + dy)$. In this paper, pair of (d_x, d_y) is presented to four directions 0^o, 45^o, 90^o and 135^o from the interest pixel (i,j) as shown in Fig.2. The matrix shows the relative frequencies $P_{i,j}$ with which two neighboring resolution cells separate by distance d, here for short $P(i,j)$ refers to GLCM which is calculated by four directions, there are eight neighbours for each pixels as shown in Fig.2.

In our research, we calculate GLCM due to these directions, the calculation of GLCM is shown in various works such as works [5] [3]. Thus, in our study, a set of welknown texture features based on GLCM are contrast, homogeneity, dissimilarity, energy, correlation, variance, inverse diference moment, entropy, sum average and sum entropy are processed in two cases study. In this paper, ten texture features are calculated from GLCM and compared the effective ones for texture of off-line signature images to figure out the most effective texture feature for off-line signature images. In detail, the information of ink contribution, the signature characteristic or pressure in the off-line texture are figured out by GLCM texture features.
The detail about the texture feature physical meaning of GLCM were presented in paper [6] and [8].

The texture features are presented as follows

$$\mu_i = \sum_{i,j=1}^{N} iP_{i,j}, \mu_j = \sum_{i,j=1}^{N} jP_{i,j}, \quad (6)$$

Contrast

$$f_1 = \sum_{i,j=1}^{N} P_{i,j}(i-j)^2, \quad (7)$$

Homogeneity

$$f_2 = \sum_{i,j=1}^{N} \frac{P_{i,j}}{1+(i-j)^2}; \quad (8)$$

Dissimilarity

$$f_3 = \sum_{i,j=1}^{N} P_{i,j}|i-j|, \quad (9)$$

Energy

$$f_4 = \sum_{i,j=1}^{N} P_{i,j}^2, \tag{10}$$

Correlation

$$f_5 = \sum_{i,j=1}^{N} i,jP(i,j)\frac{(i-\mu_i)(j-\mu j)}{\sqrt{\sigma_i \sigma j}}, \tag{11}$$

Variance

$$f_6 = \sum_{i,j=1}^{N} P_{i,j}(i-\mu i,j)^2 P_{i,j} \tag{12}$$

Inverse difference moment

$$f_7 = \sum_{i,j=1}^{N} \frac{P_{i,j}}{1+(i-j^2)}, \tag{13}$$

Entropy

$$f_8 = \sum_{i,j=1}^{N} P_{i,j}(-lnP_{i,j}), \tag{14}$$

where x and y are coordinates (row and column) of an entry in the GLCM, and $p_{x+y}(i)$ is the probability of GLCM summing to $x+y$

Sum Average

$$f_9 = \sum_{i,j=1}^{N} ip_{x+y}(i), \tag{15}$$

Sum Entropy

$$f_{10} = -\sum_{i,j=1}^{N} p_{x+y}(i)log(p_{x+y}(i)), \tag{16}$$

where i,j are index of GLCM; $P_{i,j}$ is the value of GLCM; f_l (where $l = 1,2,3...,10$) is the texture features; N is gray level of image. GLCM texture features are calculated by 4 directions, the four direction texture features are specified as $f_l(i,j,d,0^0)$, $f_l(i,j,d,45^0)$, $f_l(i,j,d,90^0)$, $f_l(i,j,d,135^0)$ with d is distance from interest pixel to its neighbors and for short they are in turn $f_l^{(0)}, f_l^{(45)}, f_l^{(90)}, f_l^{(135)}$.
These texture features of off-line signature images are calculated due to these four directions and applied in both cases which are individual texture features and a set of texture features. Fig3 indicates the comparison of GLCM contrast, dissimilarity, energy, correlation, entropy, homogeneity, variance, inverse different moment, sum average and sum entropy the first case between genuine and forgery signature images.

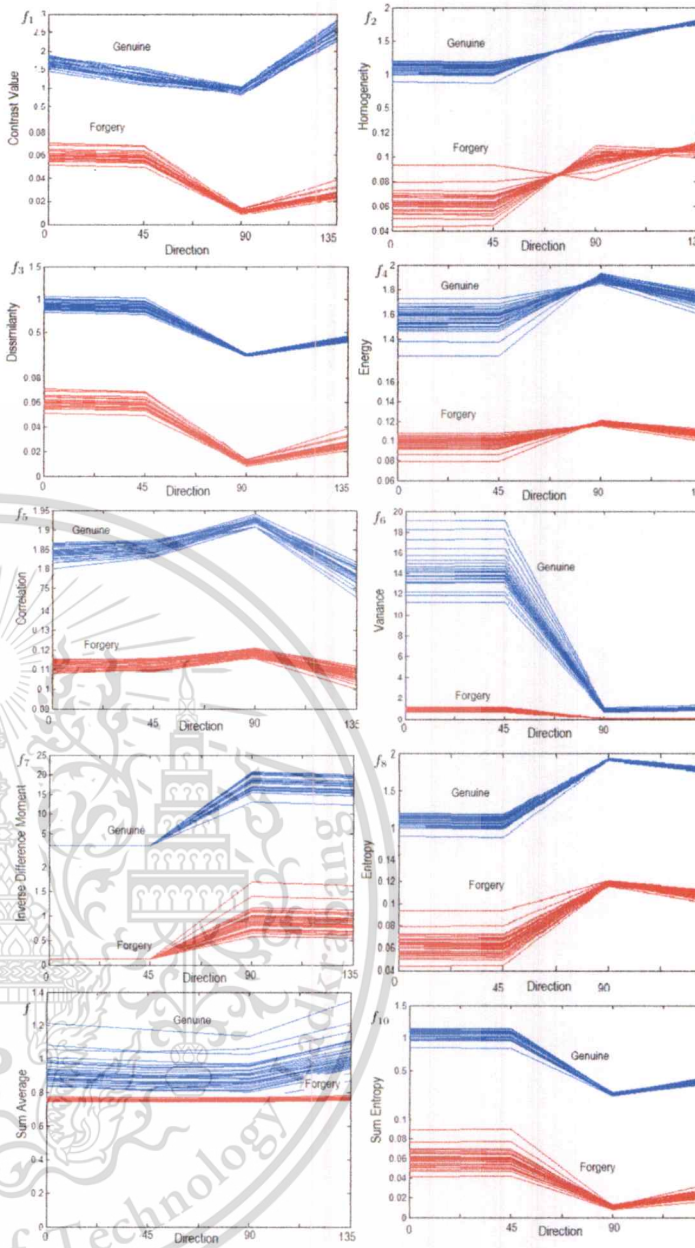

Fig. 3. Contrast, Dissimilarity, Energy, Correlation, Entropy, Homogeneity, Variance, Inverse Different Moment, Sum Average and Sum Entropy feature from genuine and forgery signature textures

IV. Signature Verification

The signature can be verified by using the texture features obtained from the previous section. The feature vector used for signature verification is defined as

$$\mathbf{f_l'} = [f_l^{(0)}, f_l^{(45)}, f_l^{(90)}, f_l^{(135)}]$$
$$\mathbf{h'} = [\mathbf{f_1'}, \mathbf{f_2'}, \mathbf{f_3'}, ..., \mathbf{f_l'}]$$

where $\mathbf{f_l}$ is the feature vector for each texture feature and $\mathbf{h}$ is a feature vector for a combination of any texture feature vector, $\mathbf{h'}$ is its transposition.
Genuine and forgery signatures are classified by prescribed Euclidean norm as follow

$$\text{Genuine if } \left\|\mathbf{h'^{(ref)}} - \mathbf{h'}\right\| < \xi, \text{ otherwise forgery.}$$

where $\mathbf{h^{ref}}$ is the reference feature vector for a particular signature. $\|.\|$ means "Euclidean norm" and ξ means prescribed threshold.

V. Experimental Result

Public database GPDS300GRAY [12] which contains 6072 genuine signatures and 7495 imitations signed by 253 signers, each signer includes 24 genuines and 30 forgery signatures is used in our experiment.

Three kinds of experiment are performed to show the effectiveness of the texture features.

In the first experiment, the feature vector $\mathbf{h}$ is defined by the individual texture feature vector $\mathbf{f}_l$ separately as

$$\mathbf{h}'_l = [\mathbf{f}'_l], (l = 1, 2, 3, ..., 10) \quad (17)$$

The experimal results obtained from the first experiment are shown in table I, the error rates rank from 6.07% to 23.9%.

In the second experiment, according to the work [13], we consider the texture features can be divided into two groups, contrast groups and orderness group. In this case, $\mathbf{h}$ in the first group and second group are defined as $\mathbf{h}'_1 = [\mathbf{f}'_1, \mathbf{f}'_2, \mathbf{f}'_3]$ and $\mathbf{h}'_2 = [\mathbf{f}'_4, \mathbf{f}'_6, \mathbf{f}'_8]$, respectively. The error rates obtain from first and second group are in turn 7.31% and 9.31%. It can be seen that the error rate obtained from contrast group is better than from the orderness group.

In the third experiment, as the result from the first experiment shows that the feature f_6 (Variance) and f_9 (Sum average) seem not suitable for off-line signature verification because their errors are higher than 10%, or even higher than 20% while others are around 6%. Therefore, $\mathbf{h}$ in the first experiment is defined as $\mathbf{h} = [\mathbf{f}'_1, \mathbf{f}'_2, \mathbf{f}'_3, \mathbf{f}'_4, \mathbf{f}'_5, \mathbf{f}'_7, \mathbf{f}'_8, \mathbf{f}'_{10}]$.

From this result comparison, we find out the effective GLCM texture features, and compare the avarage error with other works shown in table II. In this table, we show our proposed method error rate with our previous work error rate which was working on the gray level detection and another work reseached on the same database. This indicates the performance of our proposed method is better than other works with the same public database.

TABLE I
INDIVIDUAL TEXTURE FEATURES FOR OFF-LINE SIGNATURE IMAGE ERROR RATE COMPARISON IN%

No	Texture Feature	EER
f_1	Contrast	6.0738
f_2	Homogenety	6.6177
f_3	Disimilarity	6.0730
f_4	Energy	6.6073
f_5	Correlation	6.5903
f_6	Variance	14.3277
f_7	Inverse diference moment	6.6073
f_8	Entropy	6.1777
f_9	Sum average	23.9068
f_{10}	Sum entropy	6.6819

VI. Conclusion

The analysis of texture features of GLCM for off-line signature images was conducted. The wide range of texture feature were used on off-line signature with four directions to extract features from genuine and forgery signature textures. The characteristics of individual texture feature effect on off-line signature image were taken into account by two cases, the first case was individual texture feature with four directions, and the second case was the significance of set of texture features which calculated the combination characteristics of texture features on off-line signature images. The experimental results show that some texture features were not effective enough to apply for off-line signature texture image such as variance and sum average. Comparing with their physical meanings, these performances reflect that to verify genuine and forgery off-line signature image features related with randomness of texture should not be used. In addition, the error rates obtained by our method were better than our previous work and another related work with the same database.

TABLE II
ERROR RATE COMPARES WITH OTHER WORKS WHICH EXPERIMENTED ON THE SAME DATABASE%

No	Work	EER
1	Our proposed method	6.47
2	Work [1]	9.35
3	Work [4]	12.18

References

[1] P. Thumwarin, Nguyen t Minh Nguyet and T. Matsuura, *Off-line Signature Verification based on FIR System Characterizing Gray Level Change* ISST 2011 International Conference on Modelling and Simulation Techonology

[2] B. Park, Y. R. Chen, *Co-occurrence Matrix Texture Features of Multispectral Images on Poultry CarcassesAutomation and Emerging Technologies, 2001.*

[3] M. Tuceryan, A.K. Jain *Texture AnalysisThe Handbook of Pattern Recognition and Computer Vision (2nd Edition), by C. H. Chen, L. F. Pau, P. S. P. Wang (eds.), pp. 207-248, World Scientific Publishing Co., 1998*

[4] J. F. Vargas, M. A. Ferrer, C. M. Travieso and J. B. Alonso, *Off-line signature verification based on grey level information using texture features,* Proceeding of the IEEE 67(2010)375-385.

[5] R. B.Harlick, Y. Sanugam, I. Dinstein *Texture feature for image classificationIEEE Transactions on Systems, Man and Cybernetics, 1973*

[6] Park B; Chen Y R *Multispectral image co-occurrence matrix analysis for poultry carcasses inspectionTransactions of the ASAE, 39(4), 1485-1491*

[7] L. Soh and C. Tsatsoulis *Texture Analysis of SAR Sea Ice ImageryUsing Gray Level Co-Occurrence Matrices. IEEE Transactions on Geoscience Remote Sensing, vol. 37, no. 2, March 1999.*

[8] D. Gadkari *A thesis submitted in partial fulfillment of the requirements or the degree of Master of Science in Modeling and Simulatio in the College of Arts and Sciences,University of Central Florida Orlando, Florida*

[9] Lumia R; Haralick RM; Zuniga O; Shapiro L; Pong T C;Wang FP (1983) *Texture analysis of Material photographs. Pattern Recognition,*16(1), 39-46

[10] C. Sansone, M. Vento *Signature verification: increasing performance by a multistage system, Pattern Analysis & Applications*, Springer 3 (2000) 169-181

[11] K. Franke, O. B, T. S, *Ink texture analysis for writer identification* IWFHR '02: Proceedings of the Eighth International Workshop on Frontiers in Handwriting Recognition (IWFHR'02), IEEE Computer Society, Washington, DC, USA, 2002, p. 268

[12] J. F. Vargas, M. A. Ferrer, C. M. Travieso and J. B. Alonso *Off-line Handwritten Signature GPDS-960 Corpus*, in IAPR 9th International Conference on Document Analysis and Recognition, ISBN: 978-0-7695-2822.9, pp.764-768, Cutritiba, Brazil, 23-26 September 2007

[13] M. Hall-Beyer *The GLCM Tutorial Home Page*, Feb 2007